JOURNAL OF APPLIED CRYSTALLOGRAPHY

ISSN 1600-5767

MAGNDATA: towards a database of magnetic structures. II. The incommensurate case

Samuel V. Gallego,[a] J. Manuel Perez-Mato,[a]* Luis Elcoro,[a] Emre S. Tasci,[b] Robert M. Hanson,[c] Mois I. Aroyo[a] and Gotzon Madariaga[a]

[a]Departamento de Fisica de la Materia Condensada, Facultad de Ciencia y Tecnología, Universidad del País Vasco (UPV/EHU), Apartado 644, Bilbao 48080, Spain, [b]Department of Physics Engineering, Hacettepe University, Ankara 06800, Turkey, and [c]Department of Chemistry, St Olaf College, Northfield, MN 55057, USA. *Correspondence e-mail: jm.perez-mato@ehu.es

Received 1 July 2016
Accepted 3 October 2016

Edited by G. Kostorz, ETH Zurich, Switzerland

Keywords: magnetic structures database; *MAGNDATA*; incommensurate magnetic structures; magnetic superspace groups; Bilbao Crystallographic Server; superspace symmetry; irreducible representations.

A free web page under the name *MAGNDATA*, which provides detailed quantitative information on more than 400 published magnetic structures, has been made available at the Bilbao Crystallographic Server (http://www.cryst.ehu.es). It includes both commensurate and incommensurate structures. In the first article in this series, the information available on commensurate magnetic structures was presented [Gallego, Perez-Mato, Elcoro, Tasci, Hanson, Momma, Aroyo & Madariaga (2016). *J. Appl. Cryst.* **49**, 1750–1776]. In this second article, the subset of the database devoted to incommensurate magnetic structures is discussed. These structures are described using magnetic superspace groups, *i.e.* a direct extension of the non-magnetic superspace groups, which is the standard approach in the description of aperiodic crystals. The use of magnetic superspace symmetry ensures a robust and unambiguous description of both atomic positions and magnetic moments within a common unique formalism. The point-group symmetry of each structure is derived from its magnetic superspace group, and any macroscopic tensor property of interest governed by this point-group symmetry can be retrieved through direct links to other programs of the Bilbao Crystallographic Server. The fact that incommensurate magnetic structures are often reported with ambiguous or incomplete information has made it impossible to include in this collection a good number of the published structures which were initially considered. However, as a proof of concept, the published data of about 30 structures have been re-interpreted and transformed, and together with ten structures where the superspace formalism was directly employed, they form this section of *MAGNDATA*. The relevant symmetry of most of the structures could be identified with an epikernel or isotropy subgroup of one irreducible representation of the space group of the parent phase, but in some cases several irreducible representations are active. Any entry of the collection can be visualized using the online tools available on the Bilbao server or can be retrieved as a magCIF file, a file format under development by the International Union of Crystallography. These CIF-like files are supported by visualization programs like *Jmol* and by analysis programs like *JANA* and *ISODISTORT*.

1. Introduction

Under the name *MAGNDATA* we have collected on the Bilbao Crystallographic Server (http://www.cryst.ehu.es) comprehensive information on more than 400 magnetic structures, both commensurate and incommensurate. *MAGNDATA* has been developed as a proof of concept for the development of a database of magnetic structures based on the systematic application of magnetic symmetry. This task has been done within the framework of the efforts of the Commission on Magnetic Structures of the IUCr (International Union of Crystallography, 2015) for achieving a standard in the communication of magnetic structures and an

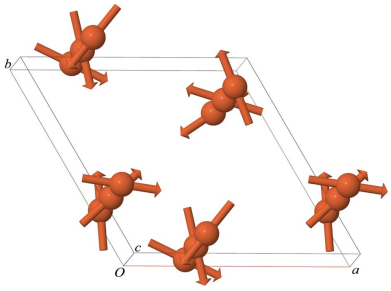

extension of the CIF format (Brown & McMahon, 2002) to magnetic structures. For a detailed description of the context under which this small database has been developed, we refer to our previous article (Gallego *et al.*, 2016), where we presented and discussed the section of *MAGNDATA* devoted to commensurate structures. This has more than 360 entries, and the structures are described within the framework of the symmetry relations described by the magnetic space groups (MSGs), also called Shubnikov groups (Litvin, 2013; Stokes & Campbell, 2011). *MAGNDATA* also includes about 40 incommensurate structures (see Fig. 1) which require a different methodology, with their symmetry being given by magnetic superspace groups (MSSGs). Here, we present and discuss the main features of this second part of the collection. We concentrate on the explanation of the information available for each structure, and the way this information can be retrieved and analysed.

The symmetry of magnetic structures with incommensurate propagation vector(s) cannot be described by an MSG (Litvin, 2013; Stokes & Campbell, 2011). Its symmetry is given instead by a superspace group (Petříček *et al.*, 2010; Perez-Mato *et al.*, 2012). The superspace formalism was developed decades ago to describe the symmetry properties of aperiodic crystals, *i.e.* incommensurate crystals and quasicrystals, and it has become the standard approach for any quantitative analysis of these systems (Janssen *et al.*, 2006, 2007; Van Smaalen, 2007; Stokes *et al.*, 2011; Janssen & Janner, 2014). Although it was clear from the beginning (Janner & Janssen, 1980) that the new concept was also extensible and applicable to incommensurate magnetic structures, superspace symmetry has been underutilized in the characterization of magnetic order until very recently, when computer programs which make use of the so-called magnetic superspace groups were developed (Petříček *et al.*, 2014; Campbell *et al.*, 2006; Perez-Mato *et al.*, 2015). Using these symmetry groups defined in a $(3 + d)$-dimensional superspace (d is the number of rationally independent propagation vectors in the modulation), incommensurately magnetic structures can be described following a crystallographic methodology, similar to the case of non-magnetic incommensurately modulated crystals and quasicrystals. For a review of the properties and application of MSSGs, see Perez-Mato *et al.* (2012). The use of magnetic superspace symmetry ensures a robust and unambiguous description of both atomic positions and magnetic moments within a common unique formalism, and this is the approach followed in *MAGNDATA*.

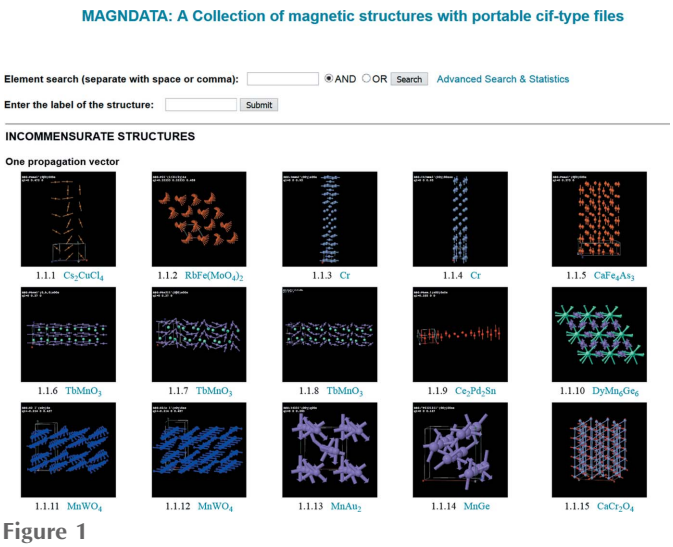

Figure 1
A screenshot, with a partial view of the online icon list of the incommensurate magnetic structures that can be retrieved from *MAGNDATA*.

The CIF format was extended years ago for the case of non-magnetic incommensurate crystals and their superspace symmetry (Brown & McMahon, 2002; Madariaga, 2005). The magCIF file format that is being developed by the Commision on Magnetic Structures of the IUCr has also extended the CIF format to incommensurate magnetic structures with the inclusion of the features associated with the MSSGs (International Union of Crystallography, 2015). We could therefore employ a preliminary version of the magCIF file format not only for commensurate magnetic structures but also for incommensurate structures. For the moment, only structures with a single rational independent incommensurate propagation vector have been included, which means that their superspace symmetry is described by a $(3 + 1)$-dimensional superspace group. Extension to structures with $(3 + d)$-dimensional superspace symmetry with $d > 1$ is, however, straightforward.

2. Description of incommensurate magnetic structures

Under the superspace formalism, the data items defining an incommensurate magnetic structure with a single rationally independent incommensurate propagation vector are the following:

(i) A unit cell that defines the average lattice periodicity of the magnetic ordering if the incommensurate modulation is taken out. This lattice acts as a reference, and its unit cell is called the basic unit cell.

(ii) A primary incommensurate propagation vector (also termed modulation wavevector in the usual superspace formalism).

(iii) The magnetic $(3 + 1)$-dimensional superspace group (MSSG), which defines the symmetry of the phase. The symmetry operations of this group define both the symmetry relations between the average positions of the atoms within the average lattice, and those between their spin, displacive and occupational modulations. These symmetry relations are expected to be satisfied within the whole thermodynamic stability range of the incommensurate phase. The fourth dimension included in these groups represents the argument of the modulation functions, and a translation along this internal coordinate corresponds to a global shift of the phase of all modulation functions.

(iv) The average atomic positions (in relative units with respect to the basic unit cell) and average magnetic moments (if the atom is magnetic) of a set of atoms in the basic unit cell that are not symmetry related and form an asymmetric unit. The average position and average magnetic moments of any

Table 1
Symmetry operations of the MSSG $P3211'(00\gamma)000s$ describing the superspace symmetry of the magnetic structure of $Ba_3NbFe_3Si_2O_{14}$ (#1.1.17; Marty *et al.*, 2008).

The MSSG label is obtained from a direct extension of the notation convention used for non-magnetic superpace groups (Janssen *et al.*, 2006), which essentially agrees with that employed by *ISODISTORT* (Campbell *et al.*, 2006) and *JANA* (Petříček *et al.*, 2014). The MSSG label included in *MAGNDATA* is only illustrative, as there are no standard labels and the group is fully defined by the provided list of symmetry operations.

N	$(x_1, x_2, x_3, x_4, \pm1)$	Seitz notation
1	$x_1, x_2, x_3, x_4, +1$	$\{1 \mid 0\}$
2	$-x_2, x_1 - x_2, x_3, x_4, +1$	$\{3^+_{001} \mid 0\}$
3	$-x_1 + x_2, -x_1, x_3, x_4, +1$	$\{3^-_{001} \mid 0\}$
4	$x_2, x_1, -x_3, -x_4, +1$	$\{2_{110} \mid 0\}$
5	$x_1 - x_2, -x_2, -x_3, -x_4, +1$	$\{2_{100} \mid 0\}$
6	$-x_1, -x_1 + x_2, -x_3, -x_4, +1$	$\{2_{010} \mid 0\}$
7	$x_1, x_2, x_3, x_4 + \frac{1}{2}, -1$	$\{1' \mid 0, 0, 0, \frac{1}{2}\}$
8	$-x_2, x_1 - x_2, x_3, x_4 + \frac{1}{2}, -1$	$\{3'^+_{001} \mid 0, 0, 0, \frac{1}{2}\}$
9	$-x_1 + x_2, -x_1, x_3, x_4 + \frac{1}{2}, -1$	$\{3'^-_{001} \mid 0, 0, 0, \frac{1}{2}\}$
10	$x_2, x_1, -x_3, -x_4 + \frac{1}{2}, -1$	$\{2'_{110} \mid 0, 0, 0, \frac{1}{2}\}$
11	$x_1 - x_2, -x_2, -x_3, -x_4 + \frac{1}{2}, -1$	$\{2'_{100} \mid 0, 0, 0, \frac{1}{2}\}$
12	$-x_1, -x_1 + x_2, -x_3, -x_4 + \frac{1}{2}, -1$	$\{2'_{010} \mid 0, 0, 0, \frac{1}{2}\}$

other atom in the unit cell can be derived from those of the asymmetric unit through the application of the symmetry operations of the MSSG defined in (iii). The term 'average' is used here to denote the periodic magnetic structure that would be obtained if the reported incommensurate modulated distortions present in the structure were cancelled. This average periodic structure, also called the basic structure in the traditional language of superspace formalism, acts as a reference for both the magnetic and structural modulations, where by construction $k = 0$ terms are not included. This average structure, usually obtained from a refinement considering all diffraction peaks, is to be distinguished from the structure that could be obtained in a refinement in which only the main reflections are used.

(v) Atomic modulation functions for the atoms in the asymmetric unit in (iv), from which the atomic modulation functions of any other atom in the basic unit cell can be derived through the application of the symmetry operations of the MSSG defined in (iii).

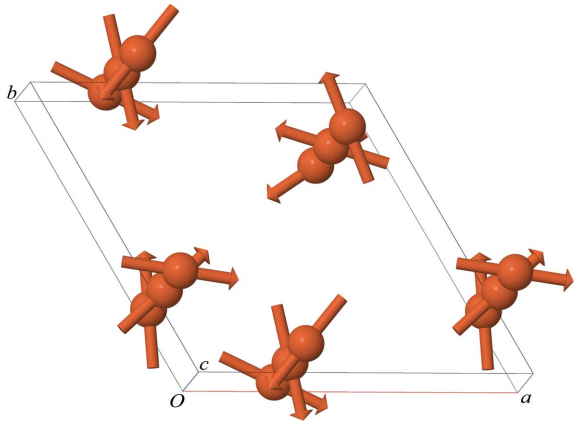

Figure 2
A schematic diagram of the incommensurate magnetic structure of $Ba_3NbFe_3Si_2O_{14}$ (Marty *et al.*, 2008), showing only the Fe atoms in three consecutive basic unit cells along **c**, as retrieved from *MAGNDATA* (#1.1.17) using its *Jmol* visualization tool.

Table 2
Average atomic positions (average magnetic moments are all zero) of symmetry-independent atoms in the incommensurate magnetic structure of $Ba_3NbFe_3Si_2O_{14}$ (#1.1.17; Marty *et al.*, 2008).

Unit cell a = 8.539 (1), b = 8.539 (1), c = 5.2414 (1) Å, α = 90, β = 90, γ = 120°, MSSG $P3211'(00\gamma)000s$ (see Table 1).

Label	Atom type	x	y	z	Multiplicity
Fe1	Fe	0.24964 (4)	0	0.5	3
Ba1	Ba	0.56598 (2)	0	0	3
Nb1	Nb	0	0	0	1
Si1	Si	0.666667	0.333333	0.5220 (1)	2
O1	O	0.666667	0.333333	0.2162 (4)	2
O2	O	0.5259 (2)	0.7024 (2)	0.3536 (3)	6
O3	O	0.7840 (2)	0.9002 (2)	0.7760 (3)	6

These five items constitute the basic information that is stored for any of the incommensurate magnetic structures gathered in *MAGNDATA* and this is the essential part of the corresponding magCIF file that can be downloaded. It should be remarked that some of the programs supporting commensurate magCIF files that were mentioned by Gallego *et al.* (2016) do not yet support magCIF files of incommensurate structures. Among those that are fully compatible, the most important ones are *Jmol* (Hanson, 2013), *ISOCIF* (Stokes & Campbell, 2014), *ISODISTORT* (Campbell *et al.*, 2006) and *JANA* (Petříček *et al.*, 2014).

As an example, Tables 1, 2 and 3 present the data available in *MAGNDATA* for the incommensurate magnetic structure of $Ba_3NbFe_3Si_2O_{14}$ reported by Marty *et al.* (2008) and depicted in Fig. 2. These data are sufficient for a full definition of this structure. The following remarks are important with respect to these data.

2.1. Symmetry operations

The list of symmetry operations (see Table 1) is the only obligatory information in a magCIF file with respect to symmetry, and it fully defines the MSSG of the structure. Operations are described with respect to the basic unit cell that defines the average lattice. They are given in a form similar to the symmetry operations of the magnetic space groups, which was explained in the previous article on the commensurate section of *MAGNDATA* (Gallego *et al.*, 2016). A direct extension of the standard notation for non-magnetic superspace groups (Janssen *et al.*, 2006) is used. Each symmetry operation is described by the transformation of a general four-dimensional position (x_1, x_2, x_3, x_4) plus the '−1/+1' symbol to indicate the inclusion or not of time reversal (second column of Table 1); this is also the format used in the magCIF files. For a better direct visualization of the operations, *MAGNDATA* also includes an alternative generalized Seitz notation (last column in Table 1), where the point-group operations are indicated with labels that can be easily interpreted (Glazer *et al.*, 2014).

Table 3
Amplitudes of the cosine and sine functions describing the spin modulation function of the only symmetry-independent magnetic atom in the incommensurate magnetic structure of $Ba_3NbFe_3Si_2O_{14}$ (#1.1.17; Marty *et al.*, 2008).

MSSG $P3211'(00\gamma)000s$ (see Table 1). **k** = (0, 0, 0.143). Magnetic moment components along the crystallographic axes are given in Bohr magnetons.

	Magnetic moment Fourier cosine coefficients						Magnetic moment Fourier sine coefficients					
	Symmetry constraints			Numerical values			Symmetry constraints			Numerical values		
Atom	x	y	z	x	y	z	x	y	z	x	y	z
Fe1	$M_{x\cos 1}$	0	0	4	0.0	0.0	$M_{x\sin 1}$	$2M_{x\sin 1}$	$M_{z\sin 1}$	−2.31	−4.62	0.0

The linear transformation of the components (x_1, x_2, x_3, x_4) associated with any symmetry operation of an MSSG can be expressed in the matrix form

$$\left(\begin{array}{ccc|c} & \mathbf{R} & & \begin{matrix}0\\0\\0\end{matrix} \\ \hline h_1 & h_2 & h_3 & R_I \end{array}\right)\begin{pmatrix} x_1 \\ x_2 \\ x_3 \\ x_4 \end{pmatrix} + \begin{pmatrix} t_1 \\ t_2 \\ t_3 \\ t_4 \end{pmatrix}, \qquad (1)$$

where **R** is a 3×3 matrix corresponding to a crystallographic three-dimensional point-group operation expressed in the basic unit-cell basis. The value of R_I (either +1 or −1) and the integers (h_1, h_2, h_3) are fully determined by **R** and the value of the incommensurate propagation vector **k** according to the relation

$$\mathbf{k}\cdot\mathbf{R} = R_I\mathbf{k} + \mathbf{H}_R, \qquad (2)$$

where $\mathbf{H}_R$ is a reciprocal lattice vector of the average structure, given by the integer components (h_1, h_2, h_3) in the reciprocal basis of the basic unit cell. In the example of Table 1, $\mathbf{H}_R$ = (0, 0, 0) for any operation. The vector $\mathbf{H}_R$ can have nonzero components (h_1, h_2, h_3) if the propagation vector lies on the Brillouin zone surface, with some commensurate fractional components. The Seitz notation for the generic operation in equation (1) is $\{\mathbf{R}' \mid t_1, t_2, t_3, t_4\}$ or $\{\mathbf{R} \mid t_1, t_2, t_3, t_4\}$, depending on the additional action of time reversal or not, where **R** now stands for the corresponding three-dimensional point-group operation. As shown in equation (2), the point-group operations present in the MSSG either keep the propagation vector invariant ($R_I = +1$) or change it to its opposite value ($R_I = -1$), in both cases modulo the basic reciprocal lattice.

2.2. Average structure

The set of operations $\{\mathbf{R} \mid t_1, t_2, t_3\}$ and $\{\mathbf{R}' \mid t_1, t_2, t_3\}$, which can be derived from the set of operations of the MSSG, define a three-dimensional MSG in the basis given by the chosen basic unit cell, which describes the symmetry of the average structure. This average structure, as an ordinary commensurate magnetic structure, is defined by the values of the atomic positions and magnetic moments of a chosen asymmetric unit (see Table 2). The three-dimensional MSG resulting from the operations in Table 1 is $P3211'$, and this is the label used as the first part of the MSSG label. It is a grey space group, as all operations are present in the group both with and without time reversal. This is the symmetry of the average structure, and therefore all average magnetic moments are necessarily zero. The list of average atomic positions for the asymmetric unit in our example is given in Table 2. As in most incommensurate structures, the average magnetic moments are forced by symmetry to be zero and are not explicitly listed. In general, if not appearing in the table they should be taken as zero. The average commensurate structure can be reconstructed from Table 2 and the given unit cell by making use of the superspace group operations listed in Table 1. The effective space group to be used can be extracted from this table.

2.3. Modulation functions

The modulation of any atomic quantity **A** for any atom with respect to its average value is in general given by a periodic modulation function (of period 1) $\mathbf{A}_\mu(x_4)$ along a single variable x_4, such that the value of the quantity **A** of atom μ in the primitive unit cell **L** is given by the value of the modulation function $\mathbf{A}_\mu(x_4)$ for $x_4 = \mathbf{k}\cdot(\mathbf{L} + \mathbf{r}_\mu)$, where $\mathbf{r}_\mu$ is the position of atom μ within the primitive unit cell. The modulation functions may be anharmonic, and they are parameterized as Fourier series in terms of cosine and sine functions. Thus, for any component i of **A**, the modulation function is defined by the real amplitudes $A_{\mu i\cos n}$ and $A_{\mu i\sin n}$ describing the modulation function in the form

$$A_{\mu i}(x_4) = \sum_n A_{\mu i\cos n}\cos(2\pi n x_4) + A_{\mu i\sin n}\sin(2\pi n x_4). \qquad (3)$$

In the case of structural modulations, a Fourier series may be ill-suited to describing the complex anharmonic modulations that are often present in aperiodic crystals, and quite a number of alternative basis functions are used for the parameterization of the modulation functions (Petříček *et al.*, 2014, 2016). In the case of magnetic modulations, however, the Fourier decomposition of equation (3) reduces in most cases to a first harmonic, or is limited to a few terms. In our example, a single harmonic is present in the spin modulation, and its Fourier cosine and sine amplitudes for the single symmetry-independent Fe atom are reproduced in Table 3.

For instance, one can see in Table 3 for our example that the cosine amplitudes of the Fe1 spin modulation are forced to be zero except for the x component, while the sine amplitudes for the x and y components are forced to have a 1:2 ratio and a z component is also allowed. This means that the amplitude of the sine modulation of the spin of the Fe atom at the position $(x, 0, \frac{1}{2})$ is on a plane perpendicular to the **a** direction, while the spin cosine modulation is along **a**. In other words, the spin modulation is forced by symmetry to follow a mixed screw/

Table 4
The set of atoms in the unit cell related by symmetry to the chosen independent magnetic atom Fe1 of $Ba_3NbFe_3Si_2O_{14}$, listed in Table 2 (#1.1.17), and the symmetry-related amplitudes of the cosine and sine functions describing their spin modulation functions, according to the MSSG $P3211'(00\gamma)000s$, defined in Table 1.

Magnetic moments are given in Bohr magnetons.

Atom	x	y	z
1	0.24964	0.00000	0.50000
2	0.00000	0.24964	0.50000
3	0.75036	0.75036	0.50000

	Magnetic moment Fourier cosine coefficients						Magnetic moment Fourier sine coefficients					
	Symmetry constraints			Numerical values			Symmetry constraints			Numerical values		
Atom	x	y	z	x	y	z	x	y	z	x	y	z
1	$M_{x\cos 1}$	0	0	4.0	0.0	0.0	$M_{x\sin 1}$	$2M_{x\sin 1}$	$M_{z\sin 1}$	−2.31	−4.62	0.0
2	0	$M_{x\cos 1}$	0	0.0	4.0	0.0	$-2M_{x\sin 1}$	$-M_{x\sin 1}$	$M_{z\sin 1}$	4.62	2.31	0.0
3	$-M_{x\cos 1}$	$-M_{x\cos 1}$	0	−4.0	−4.0	0.0	$M_{x\sin 1}$	$-M_{x\sin 1}$	$M_{z\sin 1}$	−2.31	2.31	0.0

cycloid modulation, the plane of the elliptical spin rotation being in general oblique to the propagation vector along **c**, with its plane director of type (u, $2u$, v). One can then see in Table 3 that the model reported by Marty *et al.* (2008) has additional restrictions not forced by symmetry: it is a circular screw modulation, with the plane of the spin rotation perpendicular to the **c** direction and a spin modulus of approximately 4 μ_B. This means that the amplitude of $M_{z\sin 1}$ is zero, and the nonzero values of $M_{x\sin 1}$ and $M_{y\sin 1}$ are correlated with the value of $M_{x\cos 1}$ to produce a sine component along (1, 2, 0) with the same amplitude of 4 μ_B. (Note that our parameterization has forced the inclusion of non-significant digits for these amplitudes $M_{x\sin 1}$ and $M_{y\sin 1}$). The symmetry constraints reproduced in Table 3 show that the value of $M_{x\sin 1}$ is, however, independent of $M_{x\cos 1}$, and a nonzero value of $M_{z\sin 1}$ for Fe1 is also allowed, as these additional variables do not break the superspace symmetry. Thus, the number of free parameters in the most general model of the spin modulation under this symmetry is three instead of one. Not only can the plane of rotation of the spins be oblique with respect to the propagation direction, but the rotation can also be elliptical, instead of circular. To our knowledge this more general model has never been tested, but an alternative model for the same phase has been proposed by Scagnoli *et al.* (2013). This second model indeed includes a nonzero M_z modulation. Unfortunately, some quantitative details in the description of the spin modulations seem to be missing and we have been unable to interpret the model fully and transform it to an unambiguous description within the superspace formalism. It seems, however, that the modulated spin structure proposed by Scagnoli *et al.* (2013) is not a mere improvement of the one reported by Marty *et al.* (2008), corresponding to nonzero values for the additional free variables mentioned above. The spin modulations of the structure reported by Scagnoli *et al.* (2013) do not seem to keep a constant rotation plane. Hence, its superspace symmetry must be different from that of the model proposed by Marty *et al.* (2008), and the two models are therefore in contradiction. This is a clear example where the systematic use of magnetic superspace symmetry becomes a fundamental tool in *MAGNDATA* to classify and compare different models for incommensurate magnetic structures.

2.4. Symmetry relations between modulation functions

The Fe1 site in the average structure has a multiplicity of 3, *i.e.* there are two other Fe sites within the unit cell with spin modulations that are symmetry related to that of Fe1 defined in Table 3. Optionally, *MAGNDATA* can explicitly show these symmetry-related modulations in the same format. The general equation relating the spin modulation functions of two atoms ν and μ, through an MSSG operation $\{\mathbf{R}\,|\,\mathbf{t}, t_4\}$, such that $\{\mathbf{R}\,|\,\mathbf{t}\}\mathbf{r}_\nu = \mathbf{r}_\mu$ (modulo an average lattice translation), is (see Perez-Mato *et al.*, 2012)

$$\mathbf{M}_\mu(R_I x_4 + t_4 + \mathbf{H}_R \cdot \mathbf{r}_\nu) = \pm \det(\mathbf{R})\,\mathbf{R}\mathbf{M}_\nu(x_4), \qquad (4)$$

where the parameters in equation (4) have been defined above in the context of equations (1) and (2). The ± sign depends on the operation being either $\{\mathbf{R}\,|\,\mathbf{t}, t_4\}$ or $\{\mathbf{R}'\,|\,\mathbf{t}, t_4\}$. It is important to remark that the parameterization chosen in the superspace formalism, with the correspondence between the continuous coordinate x_4 and the factor $\mathbf{k}\cdot(\mathbf{L}+\mathbf{r}_\mu)$ when particularized for a specific atom, makes the symmetry relation defined by equation (4) independent of the choice made for atoms μ and ν among those equivalent by lattice translations of the average structure. This avoids a frequent source of confusion and ambiguity in the traditional description using the factor $\mathbf{k}\cdot\mathbf{L}$. Table 4 shows the three average sites forming the orbit derived from the Fe1 site in the asymmetric unit and their corresponding modulation functions, as given in *MAGNDATA*. The table explicitly shows the relation of the modulation parameters of the two additional atoms with those of Fe1, as derived from the general equation (4). This relation forces a 120° pattern of their spins on each plane along **c**. It is important to remark that the so-called triangular chirality (Marty *et al.*, 2008) of the spin helical modulations is dictated by the MSSG, with the relation of the spin helicities of the three modulations being unique. The MSSG is chiral (as it is the space group of the paramagnetic phase) and the

enantiomeric form, which is described under the same MSSG, will have opposite chirality for both the atomic positions and the spin modulations. The helicities of all spin modulations in the enantiomeric form will be opposite but maintain their relative signs, as dictated by the MSSG. The triangular chirality defined by Marty *et al.* (2008) is therefore the same for both enantiomeric forms.

The symmetry constraints of the Fe1 spin modulation discussed in §2.3 also come from the general condition expressed by equation (4) for the operations that keep the Fe1 site invariant. The average position of this site is invariant for the operation $\{2_{100} \mid 0, 0, 0, 0\}$ (see Table 1), and equation (4) particularized for this symmetry operation yields the constraints of the Fe1 moment modulation that reduce the possible free parameters of the spin modulation from six to three.

The parameterization within the superspace formalism expressed by equation (3) essentially coincides with the traditional so-called **k**-vector description, employed for instance in the *FullProf* suite (Rodríguez-Carvajal, 1993) for incommensurate magnetic structures. The differences can be considered minor, namely the use of $\mathbf{k}\cdot(\mathbf{L}+\mathbf{r}_\mu)$ instead of $\mathbf{k}\cdot\mathbf{L}$ as the variable of the Fourier wavefunction, and the use of cosine and sine functions instead of expressing the Fourier series as complex exponentials. It is, however, the introduction of symmetry relations between the modulation functions, as given by equation (4) for each symmetry operation of the MSSG, and the resulting constraints for the modulations of atoms at special positions that make the major difference from traditional parameterization. For the sake of future reference, as the parameterization employed in *FullProf* is one of the most commonly used, we include in Appendix *A* a transcription of the symmetry relations resulting from an MSSG operation and described by equation (4) into the parameterization employed by Basireps in *FullProf*.

2.5. Assignment of the MSSG

Computer tools for the efficient application of magnetic superspace symmetry have only been made available very recently (Petříček *et al.*, 2010, 2014). Hence, the use of magnetic superspace symmetry is still rare and incommensurate magnetic structures are usually reported without controlling the possible symmetry of the model, or exploring the constraints consistent with different possible alternative MSSGs. Following the traditional representation method (Bertaut, 1968; Izyumov *et al.*, 1991), the structures are often described using basis spin functions associated with a single irreducible representation (irrep) of the parent space group, but in many cases several MSSGs are possible for a single active irrep (Perez-Mato *et al.*, 2012, 2015), and therefore the symmetry assignment becomes ambiguous if the proposed model for the spin modulations is not reported in full detail. In principle, any reported incommensurate structure can be transformed into a symmetry-based description under an MSSG, if the average structure and atomic modulations are given without ambiguity. In the worst situation, it may happen that all modulation functions are symmetry independent, and the resulting MSSG is then limited to the minimum possible superspace symmetry with its point group reduced to 1 or 11′. However, in many cases it is very difficult to extract a detailed account of all spin atomic modulations. In particular, the relative phase shifts between the spin modulations of different atoms are often absent or ambiguous in the published reports, making strenuous or even impossible the transformation of the published models into the symmetry-based unified description of this database. This has made it particularly difficult to include incommensurate structures in this collection compared with commensurate ones.

As in the commensurate case, instead of identifying the relevant MSSG with a bottom-up process, we have in most cases followed a reverse methodology, exploring the possible MSSGs for the known propagation vector and identifying the one relevant for the reported structure. For this purpose, we have used either the representation analysis tool available in *JANA* (Petříček *et al.*, 2014), which determines the possible MSSGs that can result from the action of a single irrep, or *ISODISTORT* (Campbell *et al.*, 2006), which can also determine the possible MSSGs for the cases where several irreps are active. Both programs can provide a magCIF file for each of the models corresponding to these possible alternative symmetries, and they can then be compared with the published structure. Similarly to the commensurate case (Gallego *et al.*, 2016), the relevant MSSG could be easily identified in this way in most cases, except for the above-mentioned structures where the information provided in the publication is insufficient or ambiguous. Once the MSSG was identified, the process was completed by transforming the structure and modulation parameters of the original publication to the parameterization employed in the description under this MSSG. The final model, with these transformed parameters and any convenient complementary information, was then added to a magCIF file and introduced into the database.

In most cases, a label for the MSSG is included. This is given by extending the labelling rules used for non-magnetic superspace groups, and in general it does not uniquely determine the operations of the group. An MSSG label in general has the form [SG]$(k_1, k_2, k_3)ab\ldots$, where [SG] is the standard label of the MSG of the average structure, (k_1, k_2, k_3) is a generic expression of the most general form allowed by the MSSG for the incommensurate propagation vector, and a, $b, \ldots$ are an ordered set of zeros and/or letters that define the value of t_4 that the MSSG associates with each symmetry operation represented in the label [SG], following the same order. The zeros in this set of symbols are assigned not only to the operations with $t_4 = 0$, but also to those for which $R_I = -1$, as for them the value of t_4 is not intrinsic and depends on the origin chosen along x_4. Thus, the MSSG of our example in Table 1 is $P3211'(00\gamma)000s$, indicating that the average structure has the grey MSG $P3211'$, *i.e.* it is non-magnetic, the average magnetic moments being zero. The '000*s*' at the end shows that the threefold rotation 3^+ has $t_4 = 0$, while the symbol s associated with $1'$ indicates that time reversal is

maintained combined with a $\frac{1}{2}$ translation along x_4, *i.e.* the operation $\{1' \mid 0, 0, 0, \frac{1}{2}\}$ belongs to the MSSG. For other fractional values of t_4, different letters are used following the same convention as in non-magnetic superspace groups (Janssen *et al.*, 2006).

The presence in the incommensurate propagation vector of some commensurate simple components like $\frac{1}{2}$ can introduce into the symmetry relations described by equation (4) nonzero values for the vectors $\mathbf{H}_R$. This makes the symmetry relations rather complex, with the phase shifts between modulations depending explicitly on the specific value of the atomic positions. This complication can be avoided by using a supercell for the basic structure, where the commensurate part of the propagation vector becomes a reciprocal lattice vector, and the effect of this part of the propagation vector is instead introduced by a centring of the supercell in the $(3+1)$ superspace. Thus, for instance, an incommensurate propagation vector $(\frac{1}{2}, 0, \gamma)$ on a structure with a basic primitive unit cell (a, b, c) can be replaced by $(0, 0, \gamma)$, if the basic unit cell is chosen to be $2a$, b, c and a centring $\{1 \mid \frac{1}{2}, 0, 0, \frac{1}{2}\}$ is included instead in the MSSG, which equally ensures that the modulations in two consecutive original basic unit cells along **a** have their phases shifted by π (or $\frac{1}{2}$ for x_4). If the MSSG includes this kind of centring involving internal space, the [SG] label of the basic space group has an initial letter X, instead of the usual letters employed in ordinary space groups for indicating the centring type (Janssen *et al.*, 2006).

It is important to stress that, in contrast with the non-magnetic superspace groups, there is no listing of all possible MSSGs. Therefore, there is no setting of the MSSGs that can be taken as standard. The list of the symmetry operations of the MSSG compulsorily included in a magCIF file is therefore more fundamental than in the commensurate case, in order to define the magnetic symmetry of the structure unambiguously.

In most cases, we keep as the average unit cell that of the original publication, except for cases where we have avoided the presence of commensurate components in the propagation vector through a multiplication of the reference average unit cell accompanied by appropriate centring operations, as explained above.

2.6. Ubiquity of the symmetry operation $\{1' \mid 0, 0, 0, \frac{1}{2}\}$

All single-k incommensurate structures necessarily have the symmetry operation $\{1' \mid 0, 0, 0, \frac{1}{2}\}$ within their MSSG (Perez-Mato *et al.*, 2012). This is reflected in the MSSG label by the presence of a grey magnetic space group label in the first part and an s at the end of the label. This superspace symmetry operation is due to the fact that any single harmonic modulation in any system remains invariant if the action of time reversal is followed by a global phase shift π (or $\frac{1}{2}$ in x_4 units) of the modulation. The presence of this invariance as a symmetry property of the whole phase implies the well known restriction of single-k anharmonic incommensurate magnetic structures, such that any anharmonicity of the magnetic modulation within the same thermodynamic phase can only be developed through odd harmonics. See, for instance, the case of HoMgPb (*MAGNDATA* reference #1.1.32; Lemoine *et al.*, 2012), where the third and fifth harmonics have been refined. The additional presence of a $\mathbf{k} = 0$ component or even harmonics in the magnetic modulation breaks the symmetry operation $\{1' \mid 0, 0, 0, \frac{1}{2}\}$, and this can only be explained by the independent action of two propagation vectors, with the magnetic phase thus being a $2k$ phase, although its symmetry is still described by a $(3+1)$-dimensional MSSG. This is, for instance, the case of the modulated structure reported for $DyMn_6Ge_6$ (#1.1.10; Rodriguez-Carvajal & Bouree, 2012) where, apart from the incommensurate propagation vector, a $\mathbf{k} = 0$ magnetic component has been observed and the MSSG of the structure can be labelled as $P62'2'(00\gamma)h00$ (the letter h means that $t_4 = \frac{1}{6}$ for the sixfold rotation). This is the only entry where the MSSG does not include the operation $\{1' \mid 0, 0, 0, \frac{1}{2}\}$.

2.7. Structural modulations

As in the commensurate case, the non-magnetic degrees of freedom are also subject to the magnetic symmetry group of the phase. The use of the MSSG in the parameterization of the structure makes explicit all non-magnetic degrees of freedom released by the magnetic ordering, which may be significant if the magnetoelastic coupling is strong enough. Thus, if the MSG of the average structure is lower than the parent grey group, new free parameters are present in the listing of its asymmetric unit. The MSSG in general will also allow structural modulations, which are subject to symmetry correlations analogous to those of equation (4), except for the fact that the inclusion of time reversal in the operation is irrelevant. Thus, the atomic displacive modulations (if present) of two symmetry-related atoms ν and μ must be related according to the equation

$$\mathbf{u}_\mu(R_I x_4 + t_4 + \mathbf{H}_R \cdot \mathbf{r}_\nu) = \mathbf{R}\mathbf{u}_\nu(x_4), \tag{5}$$

while for the modulation of a scalar quantity, such as the occupancy probability or the atomic charge of the sites, the following relation is required:

$$p_\mu(R_I x_4 + t_4 + \mathbf{H}_R \cdot \mathbf{r}_\nu) = p_\nu(x_4). \tag{6}$$

These equations, particularized for the operation $\{1' \mid 0, 0, 0, \frac{1}{2}\}$, imply the restriction of the structural modulations to even harmonics (Perez-Mato *et al.*, 2012). This constraint of magnetoelastic effects is often observed in single-k incommensurate magnetic structures, and its universal validity for this kind of structure becomes apparent if superspace symmetry is considered.

Even-order diffraction satellites showing the presence of magnetically induced structural modulations are often observed, but their weakness has hampered any quantitative analysis. Equations (5) and (6), however, imply that strong specific correlations between magnetic modulation and induced structural modulations should be expected, and this can help to approach the problem of its characterization.

The symmetry-dictated division between odd magnetic and even structural Fourier terms in the modulations can also happen in incommensurate magnetic structures where the

paramagnetic phase is an incommensurate structure with an intrinsic structural modulation. This is the case for CeRuSn (#1.1.35; Prokes *et al.*, 2014), where the paramagnetic phase is a monoclinic incommensurate structure with propagation vector **k** = (0, 0, 0.35) and the magnetic propagation vector is **k**/2. The resulting magnetic phase has structural and magnetic modulations complying with an MSSG for the propagation vector **k**/2, which also describes the constraints of the intrinsic structural modulation that has only even Fourier terms.

2.8. Visualization and analysis

The output page for each structure includes an image obtained using *Jmol* (Hanson, 2013) with only the magnetic atoms. A link to an online three-dimensional viewer (Perez-Mato *et al.*, 2015) that uses *JSmol*, the JavaScript version of *Jmol*, is also available (see Fig. 3). This online tool makes directly accessible the simplest and most important commands of *Jmol* through specific buttons, while the innumerable commands available to manipulate and analyse the graphical representation can be applied through a command window or a pop-up console. The visualization options include the possibility of shifting the global modulation phase both statically or dynamically (*phase shift* and *phase sliding* buttons) in order to have access to all the configurations realized along the modulation. The latest version of *Jmol* fully supports MSSGs and accepts magCIF files as input files. Therefore, the database entries can also be visualized and analysed locally using *Jmol*, provided that the user has previously downloaded this free open-source Java program.

3. Additional information

Apart from the minimal information necessary to build up the magnetic structure in three-dimensional space, *MAGNDATA* provides additional important data for each entry. This information is also included in the corresponding magCIF file that can be downloaded (local tags beyond the official magCIF dictionary are used for some of the items). We list and discuss here the most important items.

3.1. Magnetic point group

The magnetic point group associated with an incommensurate magnetic structure can be derived in a straightforward manner from the knowledge of its MSSG, simply by taking the rotation or roto-inversion operations, combined (or not) with time reversal, which are present in the group. This information is very important, as the magnetic point group governs the macroscopic crystal tensor properties. As in the commensurate case, a direct link to *MTENSOR*, another program on the Bilbao Crystallographic Server, then allows the user to explore, for this specific point group and the setting used for the structure, the symmetry constraints that should be present in the macroscopic tensorial magnetic, structural or magneto-structural properties.

3.2. Parent space group, and the relationship between the basic unit cell and the unit cell of the parent phase

Although a magnetic structure is in principle fully defined by the data discussed in the previous section, as in the commensurate case (Gallego *et al.*, 2016), the knowledge of the symmetry of its parent paramagnetic structure is fundamental to characterize the possible domains and the switching properties of the material. Therefore, this parent space group is given as additional information. Information about the relationship between the basis used for this reference parent phase and the basic unit cell employed is also included. This is

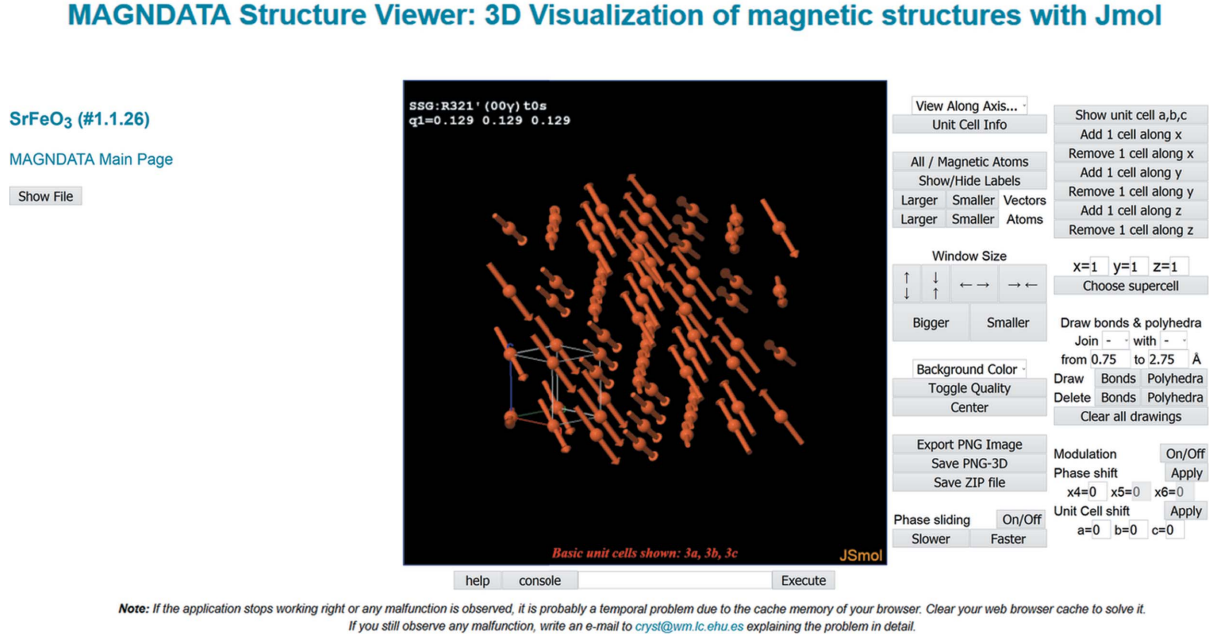

Figure 3
A screenshot of the online visualization of the incommensurate magnetic structure $SrFeO_3$ (#1.1.26; Reehuis *et al.*, 2012).

given under the heading 'Transformation from parent structure'.

If the point group of the MSSG is a strict subgroup of the point group of the parent phase, structural ferroic properties are to be expected in the incommensurate magnetic phase. Thus, for instance, in the example of $Ba_3NbFe_3Si_2O_{14}$ (#1.1.17; Marty *et al.*, 2008) the parent space group is *P*321, *i.e.* its magnetic point group is 321′, which is also the point group of the MSSG. Therefore, there is no point-group symmetry break and no distinct domains are expected, except those produced by the loss of coherence in the modulation (in 1*k* incommensurate structures, the usual trivial domains related by time reversal with opposite spins are just the same structure with its free global modulation phase shifted by π, or by $\frac{1}{2}$ in x_4 units).

On the other hand, if we take the case of $MnSb_2O_6$ (#1.1.38; Johnson *et al.*, 2013), the point-group symmetry break with respect to the parent phase is $321' \rightarrow 21'$, and domains related by the lost threefold rotation are to be expected. Note that in *MAGNDATA* we use in general for the average structure a unit-cell basis as close as possible to that of the parent space group. Thus, in this example the parent cell is maintained, and the 'Transformation from parent structure' is the identity transformation, although the monoclinic axis of the MSSG is along (1, 0, 0) of the parent trigonal lattice. In this example, knowledge of the symmetry break from a non-polar to a polar point-group symmetry is sufficient to expect this material to behave as a type II multiferroic, with a magnetically induced electric polarization along the monoclinic axis of the MSSG.

The spins in $MnSb_2O_6$ follow cycloids along the **c** direction (see Fig. 4), which is a typical geometry that introduces polarity at a local level (Perez-Mato *et al.*, 2015) and which has been identified in quite a number of incommensurate multiferroics (Tokura *et al.*, 2014). However, it is important to stress that the presence of spin cycloids is not sufficient for a polar symmetry. The symmetry of magnetic structures is a global property and there are other structures with spin cycloids, such as Cs_2CuCl_4 (#1.1.1; Coldea *et al.*, 1996), which are centrosymmetric and therefore non-polar. In this second case, the spin cycloids are related through the MSSG symmetry operations, such that the space inversion is maintained with symmetry-related cycloids of opposite chirality. In fact, in this second example, compared with the parent symmetry, one can see that the magnetic ordering does not break at all the point-group symmetry of the system (see Fig. 4).

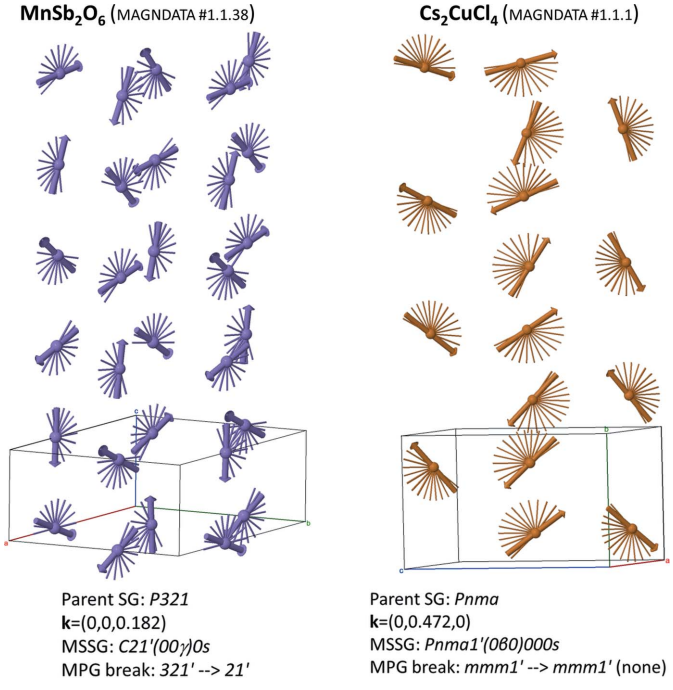

Figure 4
The spin arrangements in the magnetic structures of $MnSb_2O_6$ (#1.1.38; Johnson *et al.*, 2013) and Cs_2CuCl_4 (#1.1.1; Coldea *et al.*, 1996), as given by the online *Jmol* visualization tool of *MAGNDATA*, with an indication of their symmetry properties. Both structures exhibit spin cycloids. In the first case these produce a symmetry break into a polar symmetry, while in the second case the centrosymmetric parent point-group symmetry is maintained, through the MSSG symmetry relations between cycloids of opposite chirality. A partial trail of the spin value for a shift in the free global phase of the modulation is depicted, to show the rotation plane and chirality of each cycloid.

3.3. Representation analysis

In accordance with the Landau theory of phase transitions, the magnetic ordering in most of the magnetic phases of this collection has an order parameter transforming according to a single irrep of the parent symmetry group (odd for time reversal, when considered as a representation of the magnetic parent grey group). In fact, as mentioned above, in most cases the original structure determination was done following the traditional representation method, where the possible spin waves are restricted to a single irrep and, if necessary, the process is extended to include additional ones.

The information on the activity of one or more irreps in the spin ordering and its relation to the MSSG of the structure that is being used in the database can be found in the comments included for each entry and/or in a table with the heading 'Active irreps'. The irrep labels are those employed in *ISODISTORT*, which have also been adopted by *JANA* and by other programs on the Bilbao Crystallographic Server.

Finally, similar to the commensurate structures, each entry also includes information (if available) on the transition and experimental temperatures, references for the positional structure, and some complementary comments; see Gallego *et al.* (2016) for more details. In particular, it should also be stressed here that many incommensurate magnetic structures have been reported without providing a detailed account of the average structure that has been assumed as the reference for the modulation. In such cases, an average structure has been taken from other sources, and the corresponding reference has been included.

4. Magnetic superspace symmetry *versus* irrep descriptions

As mentioned above, in order to transform each structure to the symmetry-based unified description of this collection, its MSSG has been identified, if not given in the original refer-

ence, by exploring the possible MSSGs that can be realized if the magnetic arrangement complies with one or more irreps of the parent grey group. The MSSG that corresponds to the correlations between the spin modulations introduced in the model has then been detected.

The relation of the MSSG description to that using irreps has been discussed in detail by Perez-Mato *et al.* (2012, 2015). The database includes examples of the two different situations that can happen if a single irrep is active, given below.

(i) *A one-to-one correspondence exists between the irrep and the MSSG.* In this case, adapting the spin wave to fulfil the transformation conditions of a single irrep spin mode for the active irrep is in principle fully equivalent to the introduction of the symmetry constraints of the corresponding MSSG. However, this does *not* mean in general that the traditional form in which the representation method is being used introduces into the reported model equivalent restrictions to those of the corresponding MSSG. The reason for the difference between the two approaches in these simple cases is that the irrep-dictated transformation properties of the spin waves with respect to the operations that transform **k** into $-\mathbf{k}$ are usually disregarded. The irrep decomposition of the magnetic configuration space is usually done considering the so-called small irreps associated with the small space group $G_{\mathbf{k}}$, formed by the operations of the parent group that keep the propagation vector **k** invariant. However, the operations of the parent group that invert **k** imply in general additional restrictions on the possible form of a spin wave transforming according to a specific irrep. For instance, atomic sites related by these operations do not necessarily split [see equations (18*a*) and (18*b*) in Appendix *A*]. This problem was already pointed out within the framework of the Landau theory of some incommensurate magnetic phases (Harris *et al.*, 2008; Harris, 2007), and its relevance for a proper comparison of the superspace symmetry formalism with the representation method was discussed by Perez-Mato *et al.* (2012, 2015). In general, the MSSG symmetry properties of a single-*k* spin modulation transforming according to a single irrep are defined for all operations of what we call the extended small group $G_{\mathbf{k},-\mathbf{k}}$, which includes both the operations that maintain or invert the propagation vector.

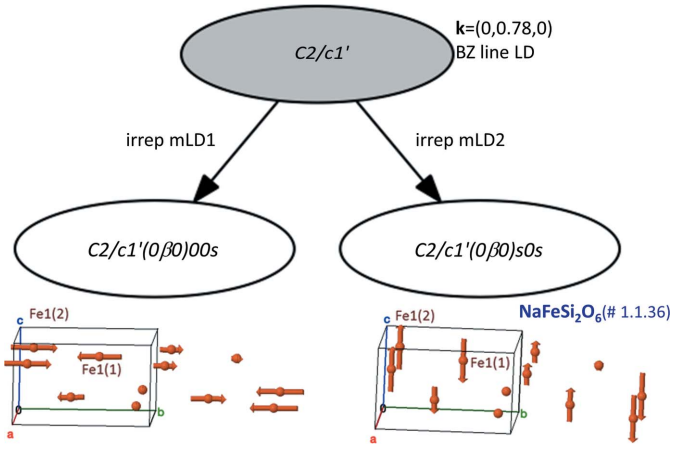

Figure 5
Possible MSSGs for an incommensurate magnetic structure with parent space group *C*2/*c* and propagation vector (0, 0.78, 0) (line LD of the BZ), resulting from the condensation of a spin wave transforming according to one of the two possible irreps. The two possible groups, one for each irrep, are depicted as maximal subgroups of the parent grey group. A partial view of the Fe spin modulation reported for $NaFeSi_2O_6$ (#1.1.36; Baum *et al.*, 2015) is represented below its MSSG, compared with the alternative model corresponding to the other irrep or MSSG. In both cases, the spin modulations of the atoms Fe1(1) and Fe1(2), which are symmetry related by the space inversion in the parent phase, keep a symmetry relation through the MSSG. While the mLD1 longitudinal wave has two free parameters to fit, the transverse mLD2 wave has four free parameters, and its collinearity is not symmetry protected. Transverse helical modulations or more complex phase relations are possible within the same irrep/MSSG.

As an example, let us consider the case of $NaFeSi_2O_6$ (#1.1.36; Baum *et al.*, 2015), which has parent space group *C*2/*c* and propagation vector (0, 0.78, 0). This propagation vector is along the Brillouin zone (BZ) line LD, with its small space group reduced to *C*2, and two possible irreps depending on the one-dimensional small irrep being even or odd for the binary rotation. The inversion and the mirror plane transform **k** into $-\mathbf{k}$, and therefore the two possible magnetic (full) irreps are two-dimensional, namely mLD1 and mLD2 in the notation of *ISODISTORT* (Campbell *et al.*, 2006). It is a general property that incommensurate spin modulations with the transformation properties of an irrep that is two-dimensional when restricted to the (**k**, $-\mathbf{k}$) subspace have superspace symmetry properties described by a single MSSG. In these cases there is a one-to-one correspondence between the irrep and this MSSG (Perez-Mato *et al.*, 2012). This is illustrated graphically in Fig. 5 for our example. Each possible irrep results in one single MSSG, and the corresponding symmetry relations and constraints on the spin waves can be derived from the general relation of equation (4).

The only symmetry-independent magnetic atom, Fe1(1), in the parent phase of $NaFeSi_2O_6$ is at Wyckoff position 4*e* (0, *y*, $\frac{1}{4}$). It is therefore invariant for the symmetry operation $\{2_{010} \mid 0, 0, \frac{1}{2}\}$. This symmetry operation is conserved either as $\{2_{010} \mid 0, 0, \frac{1}{2}, 0\}$ in the MSSG corresponding to mLD1 or as $\{2_{010} \mid 0, 0, \frac{1}{2}, \frac{1}{2}\}$ in the MSSG of mLD2. In the first case, equation (4) forces the modulation to be longitudinal with the spin constrained along the **b** direction, the first harmonic amplitudes being reduced to the two parameters $M_{y\cos 1}$ and $M_{y\sin 1}$. In the second case, *i.e.* the irrep mLD2, the operation $\{2_{010} \mid 0, 0, \frac{1}{2}, \frac{1}{2}\}$ forces a transverse modulation, with four free parameters ($M_{x\cos 1}$, 0, $M_{z\cos 1}$) and ($M_{x\sin 1}$, 0, $M_{z\sin 1}$). Both MSSGs include the inversion operation which, for a convenient choice of origin along the internal space x_4, can be expressed without any shift along x_4 as $\{-1 \mid 0, 0, 0, 0\}$. Equation (4) particularized for the inversion implies that the modulation amplitudes of Fe1(2) (see Fig. 5) are related to those of Fe1(1), in the form $M_{\alpha\cos 1}$[Fe1(2)] = $M_{\alpha\cos 1}$[Fe1(1)] and $M_{\alpha\sin 1}$[Fe1(2)] = $-M_{\alpha\sin 1}$[Fe1(1)] for $\alpha = x, y, z$, for any of the two irreps/MSSGs. Therefore, the magnetic modulation does not split the Fe sites, and both MSSGs keep a single symmetry-independent site, with two and four free parameters for mLD1 and mLD2, respectively, to describe the Fe spin modulations. For

comparison, the traditional representation approach yields four and eight parameters for the spin basis functions, respectively, which by fixing the global arbitrary phase of the incomensurate modulation reduce to three and seven.

It should be remarked that, in the MSSG description, the arbitrary global phase of the modulation is fixed by the setting used for the MSSG, if it contains operations transforming **k** into $-\mathbf{k}$. The origin along x_4 is fixed by the choice of the t_4 values of these operations. The structure of $NaFeSi_2O_6$ reported by Baum *et al.* (2015) corresponds to the MSSG $C2/c1'(0\beta0)s0s$ (irrep mLD2), but the model reported by Baum *et al.* (2015) includes additional constraints, as the spin arrangement is collinear and the number of refined parameters has been limited to three. Note however that the irrep, or equivalently the MSSG, allows more complex arrangements, including transverse helical ellipsoidal modulations.

In contrast with the commensurate case, an incommensurate spin arrangement transforming according to a single irrep, and having the MSSG symmetry associated with this irrep, can imply phase relations between the modulations of atoms that are symmetry independent in the parent space group (Perez-Mato *et al.*, 2012). This may sound paradoxical, but it is a special property of incommensurate structures and the symmetry associated with the phase shift of their modulation. In order that two incommensurate basis functions associated with symmetry-independent atoms correspond to a single spin mode transforming according to a single irrep, their relative phases should be correlated. Unfortunately, this single irrep condition, which is part of the constraints of the associated MSSG, is often not considered. This is a recurrent problem encountered when translating reported incommensurate structures into the superspace formalism. For example, the compound $CaFe_4As_3$ (#1.1.5; Manuel *et al.*, 2010) has four independent Fe sites of type 4*c* (x, $\frac{1}{4}$, z) in the parent space group *Pnma* and was reported to have centrosymmetric properties in the incommensurate phase. The irrep mY1 with **k** = (0, 0.375, 0) associated with its spin arrangement constrains the spin modulations to be longitudinal, but the transformation properties of this irrep by the inversion operation also force the modulations for the four independent Fe atoms to be in phase (Perez-Mato *et al.*, 2012). The modulation phases of the different sites were refined, however (Manuel *et al.*, 2010), and reached relative values close to zero or π, as expected from the centrosymmetric MSSG associated with a single irrep mode. Accordingly, to keep a centrosymmetric symmetry we had to ignore the small deviations from these values when introducing the structure into the database.

(ii) *Several alternative MSSGs are possible, depending on how the spin basis functions of the irrep are combined*. If the active irrep restricted to the extended small group $G_{\mathbf{k},-\mathbf{k}}$ has a dimension larger than two, more than one MSSG is in general possible, depending on the direction taken by the order parameter within the irrep space. This implies that specific linear combinations of the irrep spin basis modes can yield different MSSGs (so-called irrep epikernels), while an arbitrary combination of the whole set of basis modes reduces the symmetry to the minimum possible MSSG for the irrep (the so-called irrep kernel) (Perez-Mato *et al.*, 2012, 2015). The refined models are usually obtained by introducing *ad hoc* restrictions on the combination of irrep spin basis modes or without using irreps, simply assuming simple models following a trial-and-error approach. In many cases these restrictions make the model comply with one of the several possible MSSGs.

An example is the magnetic structure reported for $SrFeO_3$ (#1.1.26; Reehuis *et al.*, 2012), shown in Fig. 3. Having a paramagnetic cubic phase with space group $Pm\bar{3}m$, the reported magnetic structure has a propagation vector of type (u, u, u), *i.e.* it lies along the line LD of the Brillouin zone, and the active irrep is mLD3. Fig. 6 shows the group–subgroup hierarchy of all possible MSSGs which can result from the action of a magnetic order parameter transforming according to mLD3. Six different superspace symmetries are in principle possible for the magnetic phase. The magnetic atom sits at the origin, and the irrep decomposition of its magnetic representation for this propagation vector is mLD3(4) + mLD2(2), where the dimensions of the irreps restricted to the extended small group $G_{\mathbf{k},-\mathbf{k}}$ are indicated in parentheses. The subspace of mLD3-type spin configurations is therefore spanned by four independent basis modes. As shown in Fig. 6, if these modes are combined arbitrarily the superspace symmetry is reduced to a minimum triclinic group, while very specific combinations can maintain either the trigonal symmetry or centrosymmetric monoclinic symmetries with the monoclinic axis perpendicular to the propagation vector. The model reported for $SrFeO_3$ corresponds to one of these three maximum symmetries, and a single free parameter is to be refined. The magnetic modulation breaks space inversion and maintains the trigonal symmetry compatible with the propagation vector, but keeps the system non-polar owing to the binary rotations perpendicular to the propagation vector that are also preserved.

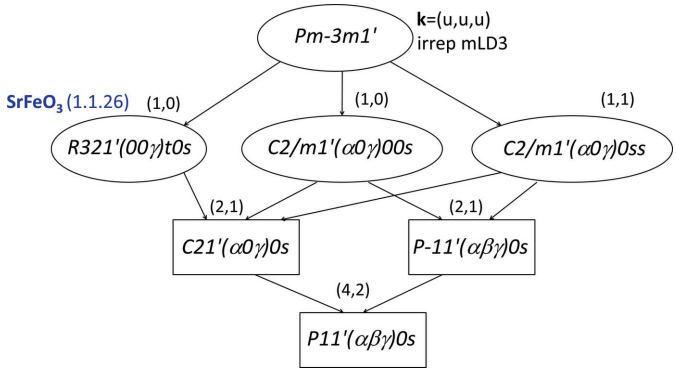

Figure 6
Possible MSSGs for an incommensurate magnetic structure with parent space group $Pm\bar{3}m$ and active irrep mLD3, with its propagation vector on the symmetry line LD (u, u, u) of the BZ. The groups are depicted showing their group–subgroup hierarchy and only one subgroup per conjugacy class is shown. The set of integers (n, m) above each group indicates the degrees of freedom of the spin wave for a magnetic atom at the origin under each symmetry, separating those associated with the irrep mLD3(n) from those with mLD2(m), these latter corresponding to possible secondary spin modes if $m \neq 0$. The MSSG of the magnetic phase of $SrFeO_3$ (#1.1.26; Reehuis *et al.*, 2012) is indicated.

As shown in Fig. 6, some of the possible MSSGs resulting from a single active irrep may have degrees of freedom associated with secondary irreps having compatible epikernels, which are supergroups of this particular MSSG. For instance, this is the case for the MSSG $C2/m1'(\alpha,0,\gamma)0ss$, which implies two free parameters in the spin modulation, but if restricted to the mLD3 irrep only one parameter is necessary, the second one corresponding to a secondary symmetry-compatible longitudinal spin component transforming according to mLD2.

The database also contains structures whose spin modulation corresponds to the superposition of two primary irreps, the resulting MSSG being the intersection of the irrep epikernels associated with each irrep. This intersection depends in general on the relative phase shift between the two irrep spin modulations (Perez-Mato *et al.*, 2012), and again various MSSGs are possible even if the two primary irreps separately result in a single possible MSSG. Among these cases, one has to include those with spin modulations corresponding to a single irrep but with arbitrary relative phase shifts between the basis functions, which decrease the resulting MSSG, breaking all operations that transform $\mathbf{k}$ into $-\mathbf{k}$. These structures must be considered the result of the action of two distinct order parameters transforming according to the same irrep. The possibility of reducing the symmetry through the superposition of irrep modes of the same irrep is a peculiarity of incommensurate structures, not present in the commensurate case.

5. Summary of the structures in the collection

Table 5 summarizes the symmetry properties of the incommensurate structures gathered in this collection. The first 13 cases in the list are structures where the magnetic point group does not vary with respect to the paramagnetic phase. No ferroic properties are therefore to be expected. No twinning can exist, not even the simple case of spin switching. In all these cases a single primary irrep is active and its small irrep is one dimensional, such that there is a one-to-one correspondence between the MSSG and the irrep; once the active irrep has been identified, the identification of the corresponding MSSG is rather straightforward. These structures have usually been refined assuming some simple form for the modulation as helical, cycloidal, sinusoidal *etc*. This kind of modulation usually complies with the MSSG associated with the active irrep, except in cases like that of $CaFe_4As_3$, discussed in the previous section, but they often include additional restrictions that are not forced by the MSSG or by the reduction to a single irrep. For instance, this is the case for $CaCr_2O_4$ (#1.1.15; Damay *et al.*, 2010), where the most general spin modulation under its MSSG is a set of elliptical cycloidal modulations with opposite chiralities by pairs and with the normal to its rotation plane being allowed to be oblique on the plane perpendicular to the propagation vector. However, the cycloids of the reported model lie on the *ac* plane, and it is not mentioned if a more general orientation was explored and checked. A similar situation occurs in the case of $Ba_3NbFe_3Si_2O_{14}$ (Marty *et al.*, 2008), discussed in §2.

The remaining structures with a single active primary irrep break the parent point-group symmetry and can be classified into three sets:

(i) Structures where the direction of the propagation vector is the only agent of this symmetry reduction, with the extended small space group $G_{\mathbf{k},-\mathbf{k}}$ being a strict subgoup of the parent space group, while the active small irrep is one dimensional. Also in these cases, there is a one-to-one correspondence between the small irrep and the MSSG, but this latter only keeps the point-group symmetry corresponding to $G_{\mathbf{k},-\mathbf{k}}$, which is lower than that of the parent phase. There are seven cases of this type.

(ii) Structures where the propagation vector does not break the parent symmetry, $G_{\mathbf{k},-\mathbf{k}}$ coinciding with the full parent space group, and the reduction of the point-group symmetry being due to the fact that the active irrep is multidimensional. This is the case for the magnetic structures of $RbFe(MoO_4)_2$ (#1.1.2), $MnAu_2$ (#1.1.13), $CeRhIn_5$ (#1.1.16), $CeAuAl_3$ (#1.1.33) and FeOCl (#1.1.40). Their MSSG is one of the epikernels of maximum symmetry of the active irrep. It is remarkable that the spin modulations in these structures are circular helical modulations and they are symmetry protected (see Fig. 7). This contrasts with other entries in the collection,

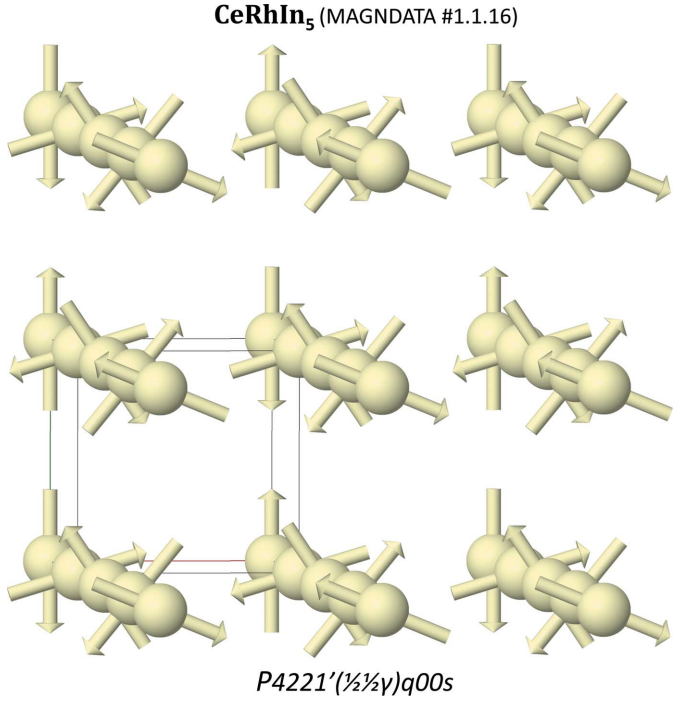

Figure 7
The incommensurate magnetic structure of $CeRhIn_5$ (#1.1.16; Bao *et al.*, 2000), with helical spin modulations that are symmetry dictated by the superspace symmetry of the phase. Only Ce atoms are shown. The label of its MSSG is indicated. The space group of the paramagnetic phase is $P4/mmm$ and the incommensurate propagation vector is of type $(\frac{1}{2},\frac{1}{2},\gamma)$. The spin modulation breaks space inversion but maintains a non-polar point-group symmetry. This MSSG is one of seven possible for the magnetic order parameter active in this phase, corresponding to a four-dimensional irrep.

Table 5
A list of the incommensurate magnetic structures included in *MAGNDATA*, with a summary of their symmetry properties.

Compounds having no point-group symmetry break are listed first. The dimension of the small irrep is given with an asterisk in those cases where the refined model includes restrictions that are not symmetry forced and apparently have not been fully assessed. Type II multiferroics are indicated with the suffix (MFII).

Material	Reference†	Parent space group	Propagation vector	Magnetic superspace group	Magnetic point group	No. of primary irreps	Dimension of small irrep
Cs_2CuCl_4 (#1.1.1)	(*a*)	*Pnma* (No. 62)	(0, 0.472, 0)	*Pnma*1′(0β0)000*s*	*mmm*1′	1	1
$CaFe_4As_3$ (#1.1.5)	(*b*)	*Pnma* (No. 62)	(0, 0.475, 0)	*Pnma*1′(0β0)000*s*	*mmm*1′	1	1
$TbMnO_3$ (#1.1.6)	(*c*)	*Pbnm* (No. 62)	(0, 0.27, 0)	*Pbnm*1′(0β0)*s*00*s*	*mmm*1′	1	1*
$MnWO_4$ (#1.1.12)	(*d*)	*P*2/*c* (No. 13)	(−0.214, 0, 0.457)	*X*2/*c*1′(α0γ)0*ss*	2/*m*1′	1	1
$CaCr_2O_4$ (#1.1.15)	(*e*)	*Pbnm* (No. 62)	(0, 0, 0.477)	*Pbnm*1′(00γ)*s*00*s*	*mmm*1′	1	1*
$Ba_3NbFe_3Si_2O_{14}$ (#1.1.17)	(*f*)	*P*321 (No. 150)	(0, 0, 0.143)	*P*3211′(00γ)000*s*	321′	1	1*
$NdFe_3B_4O_{12}$ (#1.1.18)	(*g*)	*R*32 (No. 155)	(0, 0, 1.502)	*R*321′(00γ)*t*0*s*	321′	1	1
UPtGe (#1.1.19)	(*h*)	*Imm*2 (No. 44)	(0.554 (1), 0, 0)	*Imm*21′(α00)0*s*0*s*	*mm*21′	1	1
Li_2IrO_3 (#1.1.20)	(*i*)	*Fddd* (No. 70)	(0.5768 (3), 0, 0)	*Fddd*1′(α00)0*s*0*s*	*mmm*1′	1	1
$PrNi_2Si_2$ (#1.1.34)	(*j*)	*I*4/*mmm* (No. 139)	(0, 0, 0.87)	*I*4/*mmm*1′(00γ)00*sss*	4/*mmm*1′	1	1
CeRuSn (#1.1.35)	(*k*)	*C*2/*m* (No. 12)	(0, 0, 0.175)	*C*2/*m*1′(α0γ)0*ss*	2/*m*1′	1	1
$NaFeSi_2O_6$ (#1.1.36)	(*l*)	*C*2/*c* (No. 15)	(0, 0.78, 0)	*C*2/*c*1′(0β0)*s*0*s*	2/*m*1′	1	1*
$Ca_3Co_2O_6$ (#1.1.39)	(*m*)	*R*$\bar{3}$*c* (No. 167)	(0, 0, 1.02)	*R*$\bar{3}$*c*1′(00γ)00*s*	$\bar{3}$*m*1′	1	1
Cr (#1.1.4)	(*n*)	*Im*$\bar{3}$*m* (No. 229)	(0, 0, 0.95)	*I*4/*mmm*1′(00γ)00*sss*	4/*mmm*1′	1	1
Ce_2Pd_2Sn (#1.1.9)	(*o*)	*P*4/*mbm* (No. 127)	(0.105, 0, 0)	*Pbam*1′(α00)0*s*0*s*	*mmm*1′	1	1
MnGe (#1.1.14)	(*p*)	$P2_13$ (No. 198)	(0, 0, 0.167 (4))	*P*2121211′(00γ)00*ss*	2221′	1	1*
$TmCu_2Ge_2$ (#1.1.23)	(*q*)	*I*4/*mmm* (No. 139)	(0.117, 0.117, 0)	*Fmmm*1′(α00)0*s*0*s*	*mmm*1′	1	1
CeMgPb (#1.1.27)	(*r*)	*I*4/*mmm* (No. 139)	(0.448, $\frac{1}{2}$, 0)	*I*112/*m*1′($\alpha\beta$0)00*s*	2/*m*1′	1	1*
TmMgPb (#1.1.28)	(*r*)	*I*4/*mmm* (No. 139)	(0.412, 0, 0)	*Immm*1′(α00)0*s*0*s*	*mmm*1′	1	1
ErMgPb (#1.1.29)	(*r*)	*I*4/*mmm* (No. 139)	(0.816, 0, 0)	*Immm*1′(α00)0*sss*	*mmm*1′	1	1
$RbFe(MoO_4)_2$ (#1.1.2) (MFII)	(*s*)	*P*$\bar{3}$ (No. 147)	($\frac{1}{3}$, $\frac{1}{3}$, 0.458)	*P*31′($\frac{11}{33}\gamma$)*ts*	31′	1	2
$MnAu_2$ (#1.1.13)	(*t*)	*I*4/*mmm* (No. 139)	(0, 0, 0.283)	*I*4221′(00γ)*q*00*s*	4221′	1	2
$CeRhIn_5$ (#1.1.16)	(*u*)	*I*4/*mmm* (No. 139)	($\frac{1}{2}$, $\frac{1}{2}$, 0.297)	*P*4221′($\frac{11}{22}\gamma$)*q*00*s*	4221′	1	2
$CeAuAl_3$ (#1.1.33)	(*v*)	*I*4*mm* (No. 107)	(0, 0, 0.52)	*I*41′(00γ)*qs*	41′	1	2
FeOCl (#1.1.40)	(*w*)	*Pmmn* (No. 59)	(0.286, $\frac{1}{2}$, 0)	*X*2/*n*1′($\alpha\beta$0)00*s*	2/*m*1′	1*	2
Cr (#1.1.3)	(*n*)	*Im*$\bar{3}$*m* (No. 229)	(0, 0, 0.95)	*Immm*1′(00γ)*s*00*s*	*mmm*1′	1	2
$SrFeO_3$ (#1.1.26)	(*x*)	*Pm*$\bar{3}$*m* (No. 221)	(0.129, 0.129, 0.129)	*R*321′(00γ)*t*0*s*	321′	1	2
$TbMnO_3$ (#1.1.7) (MFII)	(*c*)	*Pbnm* (No. 62)	(0, 0.27, 0)	*Pbn*211′(0β0)*s*00*s*	*mm*21′	2	1, 1
$TbMnO_3$ (#1.1.8) (MFII)	(*c*)	*Pbnm* (No. 62)	(0, 0.27, 0)	*Pbn*211′(0β0)*s*00*s*	*mm*21′	2	1, 1
$MnWO_4$ (#1.1.11) (MFII)	(*d*)	*P*2/*c* (No. 13)	(−0.214, 0, 0.457)	*X*21′(α0γ)0*s*	21′	2	1, 1
Li_2IrO_3 (#1.1.21)	(*y*)	*Cccm* (No. 66)	(0.57 (1), 0, 0)	*C*2221′(α00)*s*00*s*	2221′	2*	1, 1
$Sr_3Fe_2O_7$ (#1.1.22)	(*z*)	*Im*$\bar{3}$*m* (No. 229)	(0.1416, 0.1416, 0)	*X*2221′($\alpha\alpha$0)*s*00*s*	2221′	2*	1, 1
CrAs (#1.1.24)	(*aa*)	*Pnma* (No. 62)	(0, 0, 3562)	*P*2121211′(00γ)00*ss*	2221′	2*	1, 1
TbMgPb (#1.1.30)	(*r*)	*I*4/*mmm* (No. 139)	(0.843 (1), 0, 0)	*I*2/*m*1′($\alpha\beta$0)00*s*	2/*m*1′	2	1, 1
DyMgPb (#1.1.31)	(*r*)	*I*4/*mmm* (No. 139)	(0.841 (1), 0.016 (1), 0)	*I*2/*m*1′($\alpha\beta$0)00*s*	2/*m*1′	2	1, 1
HoMgPb (#1.1.32)	(*r*)	*I*4/*mmm* (No. 139)	(0.835, 0, 0)	*I*2/*m*1′($\alpha\beta$0)00*s*	2/*m*1′	2	1, 1
$MnSb_2O_6$ (#1.1.38) (MFII)	(*bb*)	*P*321 (No. 150)	(0, 0, 0.182)	*C*21′(00γ)0*s*	21′	2	1, 1
$LiFeAs_2O_7$ (#1.1.25)	(*cc*)	*C*2 (No. 5)	(0.709, 0, 0.155)	*C*11′($\alpha\beta\gamma$)0*s*	11′	2 (2×1)	1, 1
$NaFeSi_2O_6$ (#1.1.37) (MFII)	(*l*)	*C*2/*c* (No. 15)	(0, 0.78, 0)	*C*21′(0β0)*ss*	21′	2 (2×1)	1, 1
$DyMn_6Ge_6$ (#1.1.10)	(*o*)	*P*6/*mmm* (No. 191)	(0, 0, 0.1651)	*P*62′2′(00γ)*h*00	62′2′	2	2, 1

† References for the magnetic structures: (*a*) Coldea *et al.* (1996), (*b*) Manuel *et al.* (2010), (*c*) Kenzelmann *et al.* (2005), (*d*) Urcelay-Olabarria *et al.* (2013), (*e*) Damay *et al.* (2010), (*f*) Marty *et al.* (2008), (*g*) Janoschek *et al.* (2010), (*h*) Mannix *et al.* (2000), (*i*) Biffin, Johnson, Choi *et al.* (2014), (*j*) Blanco *et al.* (2010), (*k*) Prokes *et al.* (2014), (*l*) Baum *et al.* (2015), (*m*) Agrestini *et al.* (2008), (*n*) Perez-Mato *et al.* (2012), (*o*) Rodriguez-Carvajal & Bouree (2012), (*p*) Makarova *et al.* (2012), (*q*) Penc *et al.* (2012), (*r*) Lemoine *et al.* (2012), (*s*) Kenzelmann *et al.* (2007), (*t*) Herpin & Meriel (1961), (*u*) Bao *et al.* (2000), (*v*) Adroja *et al.* (2015), (*w*) Hwang *et al.* (2000), (*x*) Reehuis *et al.* (2012), (*y*) Biffin, Johnson, Kimchi *et al.* (2014), (*z*) Kim *et al.* (2014), (*aa*) Keller *et al.* (2015), (*bb*) Johnson *et al.* (2013), (*cc*) Rousse *et al.* (2013).

where the regular spin helical or cycloidal spin arrangement which has been reported is not symmetry dictated and other more complex arrangements are possible for the same irrep and the same MSSG. For instance, this is the case for MnGe (#1.1.14; Makarova *et al.*, 2012), where the Mn atom occupies a general position and therefore its spin modulation has no symmetry restriction, while the refinement was done assuming pure helical modulations.

The case of FeOCl (#1.1.40) within this set is also representative of the problems that have arisen when transforming the published structures into an unambiguous symmetry-based description. According to our interpretation, the figures in the publication show spin cycloids with chiralities that are inconsistent with the corresponding equations in the text. We therefore had to decide which of the two representations was the correct one, and finally considered the equations to be more reliable.

(iii) Structures where the propagation vector and a multi-dimensional irrep are both agents of the point-group symmetry break. This is the case for $SrFeO_3$ (#1.1.26), discussed in the previous section, and also for Cr (#1.1.3).

The remaining 13 structures involve the presence of spin modulations according to two irreps. In all cases except one, the two irreps refer to the same propagation vector. The superposition of two irreps implies in general a drastic symmetry reduction. This set includes those structures where the symmetry reduction takes place through the superposition of two spin modes transforming according to the same irrep,

mentioned in the previous section. Two cases of this type have been collected, namely $LiFeAs_2O_7$ (# 1.1.25) and $NaFeSi_2O_6$ (#1.1.37). In the case of $NaFeSi_2O_6$ (Baum *et al.*, 2015), the condensation of two independent order parameters transforming according to the same irrep seems well established, as this phase is preceded by another one with a single order parameter belonging to this irrep (see #1.1.36). In contrast, the model of $NaFeSi_2O_6$ (#1.1.37) was derived following the traditional representation method, where irrep restrictions coming from the operations transforming $\mathbf{k}$ into $-\mathbf{k}$ are not considered, and a more symmetrical model with a single irrep order parameter was not tested.

The last structure in the list, $DyMn_6Ge_6$ (#1.1.10), is the only case where the incommensurate irrep superposes with a $\mathbf{k} = 0$ spin modulation. As mentioned above, this implies that the operation $\{1' \mid 0, 0, 0, \frac{1}{2}\}$, present in all other structures, is absent, and the MSG of the average structure does not include the time-reversal operation. In contrast with all the other cases, the atomic magnetic moments therefore have nonzero average values. Typical incommensurate systems belonging to this class, with an additional $\mathbf{k} = 0$ spin mode and a non-grey point-group symmetry, are all structures with conical spin modulations.

The magnetic point-group symmetry change between the paramagnetic and magnetic structures listed in Table 5 for each structure governs its possible ferroic properties. In particular, a symmetry break from a non-polar to a polar point-group symmetry is sufficient to have the symmetry conditions for a type II multiferroic, if it is an insulator. In general, a necessary (but not sufficient) condition for a non-polar/polar symmetry break is either a multidimensional small irrep for the magnetic order parameter, or the presence of two or more primary irreps, if their small irrep is one dimensional. As shown in Table 5, this collection includes five type II multiferroics. In four of them the symmetry break involves the superposition of two primary irreps ($TbMnO_3$, $MnWO_4$, $MnSb_2O_6$ and $NaFeSi_2O_6$), and only in the case of $RbFe(MO_4)_2$ is a single multidimensional primary irrep active (actually, it is a physically irreducible representation). It is important to stress that the multiferroic character of these phases can be derived directly from knowledge of the magnetic point group of the magnetic structure compared with that of the paramagnetic phase, without appealing to any particular mechanism. An additional important fact to note is that the presence of the symmetry operation $\{1' \mid 0, 0, 0, \frac{1}{2}\}$ in all single-k incommensurate structures precludes the existence in these phases of any linear magnetoelectric or magnetoelastic effect within a single domain, the magnetic point-group of these phases being grey.

6. Conclusions

As a final word of caution, we should stress that the transformation to the unambiguous quantitative description used in this database has in many cases required an exercise in the interpretation of the tables, equations and/or figures in the original publications, and this may have been incorrect. Often, some clear ambiguities or inconsistencies were detected in the data, and the transformation of the proposed structure to a fully unambiguous description under a certain MSSG required some additional assumptions on our part. In such cases, comments describing the problem are included both on the entry web page and in the magCIF file. Our interpretation of some of the publications may therefore be defective and we would greatly appreciate any report of such types of problem.

Finally, we stress, as we did in our previous paper (Gallego *et al.*, 2016), that this collection does not pretend to become a complete and updated database of all published incommensurate magnetic structures. We lack the means for such an endeavour. However, we hope that this work will stimulate further efforts within the community in the direction of the standardization and unambiguous communication of incommensurate magnetic structures through files in magCIF format, with the aim of making such a database possible in the not-too-distant future. Meanwhile, authors having published any incommensurate magnetic structure that is absent from this collection, and who are interested in having it included, are invited to contact us through the given email address.

APPENDIX *A*
Superspace symmetry relations using the parameterization of *FullProf*

In the superspace description, for single-k modulations, the spin modulation of a representative atom ν in the unit cell of the basic structure is expressed as

$$\mathbf{M}^{\nu}(x_4) = \mathbf{M}_0^{\nu} + \sum_{n=1,\ldots} \left[\mathbf{M}_{\sin n}^{\nu} \sin(2\pi n x_4) + \mathbf{M}_{\cos n}^{\nu} \cos(2\pi n x_4)\right], \tag{7}$$

with the value of the magnetic moment $\mathbf{M}_{\mathbf{L}}^{\nu}$ of atom ν in unit cell $\mathbf{L}$ being given by

$$\mathbf{M}_{\mathbf{L}}^{\nu} = \mathbf{M}^{\nu}\left[x_4 = \mathbf{q}\cdot(\mathbf{L} + \mathbf{r}_{\nu})\right]. \tag{8}$$

Here $\mathbf{k}$ is the propagation vector and $\mathbf{r}_{\nu}$ is the position of atom ν within the unit cell. All quantities are real, and they are decomposed into three components along the crystallographic directions:

$$\begin{aligned} \mathbf{M}_{\sin n}^{\nu} &= \left(M_{x\sin n}^{\nu}, M_{y\sin n}^{\nu}, M_{z\sin n}^{\nu}\right), \\ \mathbf{M}_{\cos n}^{\nu} &= \left(M_{x\cos n}^{\nu}, M_{y\cos n}^{\nu}, M_{z\cos n}^{\nu}\right). \end{aligned} \tag{9}$$

In *FullProf* (Basireps), this spin modulation is expressed instead as

$$\mathbf{M}_{\mathbf{L}}^{\nu} = \mathbf{M}_0^{\nu} + \sum_{n}\left[\mathbf{S}_{n\mathbf{k}}^{\nu} \exp\left(-i2\pi n\mathbf{k}\cdot\mathbf{L}\right) + \mathbf{S}_{n\mathbf{k}}^{\nu *} \exp\left(i2\pi n\mathbf{k}\cdot\mathbf{L}\right)\right]. \tag{10}$$

Note the explicit minus sign for the Fourier amplitude $\mathbf{S}_{\mathbf{k}}^{\nu}$ associated with $\mathbf{k}$. Comparing the two expressions, the following relation exists between the two types of parameter:

$$2\mathbf{S}_{n\mathbf{k}}^{\nu} \exp\left(i2\pi n\mathbf{k}\cdot\mathbf{r}_{\nu}\right) = \mathbf{M}_{\cos n}^{\nu} + i\mathbf{M}_{\sin n}^{\nu}, \tag{11}$$

and for a single harmonic

$$2\mathbf{S}_{\mathbf{k}}^{\nu}\exp(i2\pi\mathbf{k}\cdot\mathbf{r}_{\nu})=\mathbf{M}_{\cos 1}^{\nu}+i\mathbf{M}_{\sin 1}^{\nu}. \quad (12)$$

If we call

$$\mathbf{S}_{\mathbf{k}}^{\nu}=\left[S(\mathbf{k})_{x}^{\nu},S(\mathbf{k})_{y}^{\nu},S(\mathbf{k})_{z}^{\nu}\right], \quad (13)$$

then

$$\begin{aligned}\mathbf{M}_{\cos 1}^{\nu}&=2\mathrm{Re}\left\{\left[S(\mathbf{k})_{x}^{\nu},S(\mathbf{k})_{y}^{\nu},S(\mathbf{k})_{z}^{\nu}\right]\exp(i2\pi\mathbf{k}\cdot\mathbf{r}_{\nu})\right\},\\ \mathbf{M}_{\sin 1}^{\nu}&=2\mathrm{Im}\left\{\left[S(\mathbf{k})_{x}^{\nu},S(\mathbf{k})_{y}^{\nu},S(\mathbf{k})_{z}^{\nu}\right]\exp(i2\pi\mathbf{k}\cdot\mathbf{r}_{\nu})\right\}.\end{aligned} \quad (14)$$

If $\{\mathbf{R},\theta\mid\mathbf{t},t_4\}$ is a symmetry operation, where θ is -1 or $+1$ depending on whether the operation includes time reversal or not, and a second atom μ is related to atom ν such that $\{\mathbf{R}\mid\mathbf{t}\}\,\mathbf{r}_{\nu}=\mathbf{r}_{\mu}+\mathbf{L}$ (with $\mathbf{L}$ some particular lattice translation), then the Fourier amplitudes of atom μ are related to those of atom ν by

$$\mathbf{M}^{\mu}(R_{\mathrm{I}}x_4+t_4+\mathbf{H}_{\mathrm{R}}\cdot\mathbf{r}_{\nu})=\theta\det(\mathbf{R})\,\mathbf{R}\cdot\mathbf{M}^{\nu}(x_4), \quad (15)$$

where R_{I} (+1 or −1) and the reciprocal lattice vector $\mathbf{H}_{\mathrm{R}}$ are defined by the relation

$$\mathbf{k}\cdot\mathbf{R}=R_{\mathrm{I}}\mathbf{k}+\mathbf{H}_{\mathrm{R}}. \quad (16)$$

Equation (15) implies that

$$\begin{aligned}\mathbf{M}_{\cos 1}^{\mu}+i\mathbf{M}_{\sin 1}^{\mu}=&\exp\left[i2\pi(t_4+\mathbf{H}_{\mathrm{R}}\cdot\mathbf{r}_{\nu})\right]\\ &\times\theta\det(\mathbf{R})\,\mathbf{R}\cdot\left(\mathbf{M}_{\cos 1}^{\nu}+R_{\mathrm{I}}i\mathbf{M}_{\sin 1}^{\mu}\right),\end{aligned} \quad (17)$$

or, in terms of the *FullProf* (Basireps) parameters,

$$\begin{aligned}\mathbf{S}_{\mathbf{k}}^{\mu}=&\theta\det(\mathbf{R})\,\mathbf{R}\mathbf{S}_{\mathbf{k}}^{\nu}\exp\left[-i2\pi\mathbf{k}\cdot\left(\mathbf{r}_{\mu}-\mathbf{r}_{\nu}\right)\right]\\ &\times\exp\left[i2\pi(t_4+\mathbf{H}_{\mathrm{R}}\cdot\mathbf{r}_{\nu})\right],\end{aligned} \quad (18a)$$

if $R_{\mathrm{I}}=+1$, and

$$\begin{aligned}\mathbf{S}_{\mathbf{k}}^{\mu}=&\theta\det(\mathbf{R})\,\mathbf{R}\mathbf{S}_{\mathbf{k}}^{\nu*}\exp\left[-i2\pi\mathbf{k}\cdot\left(\mathbf{r}_{\mu}+\mathbf{r}_{\nu}\right)\right]\\ &\times\exp\left[i2\pi(t_4+\mathbf{H}_{\mathrm{R}}\cdot\mathbf{r}_{\nu})\right],\end{aligned} \quad (18b)$$

if $R_{\mathrm{I}}=-1$.

However, the two atomic positions are related in the form

$$\mathbf{k}\cdot\mathbf{r}_{\mu}-R_{\mathrm{I}}\mathbf{k}\cdot\mathbf{r}_{\nu}=\mathbf{k}\cdot\mathbf{t}+\mathbf{H}_{\mathrm{R}}\cdot\mathbf{r}_{\nu}. \quad (19)$$

Equations (18*a*) and (18*b*) can then be put as

$$\mathbf{S}_{\mathbf{k}}^{\mu}=\theta\det(\mathbf{R})\,\mathbf{R}\mathbf{S}_{\mathbf{k}}^{\nu}\exp(-i2\pi\mathbf{k}\cdot\mathbf{t})\exp(i2\pi t_4), \quad (20a)$$

if $R_{\mathrm{I}}=+1$, and

$$\mathbf{S}_{\mathbf{k}}^{\mu}=\theta\det(\mathbf{R})\,\mathbf{R}\mathbf{S}_{\mathbf{k}}^{\nu*}\exp(-i2\pi\mathbf{k}\cdot\mathbf{t})\exp(i2\pi t_4), \quad (20b)$$

if $R_{\mathrm{I}}=-1$.

Note that these equations depend on the value of $\mathbf{t}$ in $\{\mathbf{R}\mid\mathbf{t}\}$, which implies a dependence on the choice made for atom μ among the set of atoms equivalent by lattice translations of the basic structure. Equations (20*a*) and (20*b*) can be used to introduce a certain superspace symmetry operation when using *FullProf* (Basireps), but it has to be applied systematically, including all atoms in an orbit and all the operations of the superspace group.

A1. Example: inversion operation

If the system has an inversion centre $\{-1\mid0,0,0,0\}$ and two atoms are related by this inversion operation, so that $\mathbf{r}_{\mu}=-\mathbf{r}_{\nu}$, then their Fourier amplitudes according to equations (20*a*) and (20*b*) must be related in the form

$$\mathbf{S}_{\mathbf{k}}^{\mu}=\mathbf{S}_{\mathbf{k}}^{\nu*}. \quad (21)$$

However, if by convenience one is using as a representative for atoms μ the atom fulfilling $\mathbf{r}_{\mu}=-\mathbf{r}_{\nu}+(1,0,0)$, then $\{\mathbf{R}\mid\mathbf{t}\}$ in equations (20*a*) and (20*b*) becomes $\{-1\mid1,0,0\}$ and the relation of equation (21) must be changed to

$$\mathbf{S}_{\mathbf{k}}^{\mu}=\mathbf{S}_{\mathbf{k}}^{\nu*}\exp[-i2\pi\mathbf{k}\cdot(1,0,0)]. \quad (22)$$

This dependence on the atom representative is not present in the superspace parameterization, where for any $\mathbf{k}$ which does not include commensurate components making $\mathbf{H}_{\mathrm{R}}\neq0$ the relation is

$$\begin{aligned}\mathbf{M}_{\cos 1}^{\mu}&=\mathbf{M}_{\cos 1}^{\nu},\\ \mathbf{M}_{\sin 1}^{\mu}&=-\mathbf{M}_{\sin 1}^{\nu}.\end{aligned} \quad (23)$$

If the inversion centre and atom ν lie at the origin, such that $\mu=\nu$ for $\{-1\mid0,0,0,0\}$, then its spin Fourier amplitude should be real:

$$\mathbf{S}_{\mathbf{k}}^{\mu}=\mathbf{S}_{\mathbf{k}}^{\mu*}. \quad (24)$$

However, if atom ν lies at $(\frac{1}{2},0,0)$, then the relevant MSSG operation is $\{-1\mid1,0,0,0\}$ and the same phase factor as in equation (22) appears. This phase shift only implies that, in fact, all modulations for atoms lying on inversion centres are in phase, considering their relative positions. Indeed, in the superspace parameterization, the invariance of atom μ for an MSSG operation $\{-1\mid\mathbf{t},0\}$, whatever the value of $\mathbf{t}$, implies that $\mathbf{M}_{\sin 1}^{\mu}=0$ (if $\mathbf{H}_{\mathrm{R}}=0$). The application of the MSSG operations transforming $\mathbf{k}$ into $-\mathbf{k}$ with a given value of t_4 implies a specific choice of the global phase of the modulation. As this phase is arbitrary, the important result is that all atoms lying on inversion centres should be in phase.

Acknowledgements

The authors thank Branton Campbell and Harold Stokes for very helpful and fruitful interactions. The use of their program *ISODISTORT* and its constant improvements and extensions have been fundamental for the realization of this work. We are also indebted to V. Petříček for introducing the magCIF format into the communication tools of his program *JANA* which, as explained above, was used extensively to produce preliminary magCIF files of the structures. Very helpful comments and suggestions from Juan Rodriguez-Carvajal are also gratefully acknowledged. One of us (JMPM) is also especially indebted to J. L. Ribeiro for helpful comments and interchange of information in the early stages of this work. This work was supported by the Spanish Ministry of Economy and Competitiveness and FEDER funds (project Nos. MAT2012-34740 and MAT2015-66441-P) and the Government of the Basque Country (project IT779-13).

References

Adroja, D. T., de la Fuente, C., Fraile, A., Hillier, A. D., Daoud-Aladine, A., Kockelmann, W., Taylor, J. W., Koza, M. M., Burzurí,

E., Luis, F., Arnaudas, J. I. & del Moral, A. (2015). *Phys. Rev. B*, **91**, 134425.
Agrestini, S., Chapon, L. C., Daoud-Aladine, A., Schefer, J., Gukasov, A., Mazzoli, C., Lees, M. R. & Petrenko, O. A. (2008). *Phys. Rev. Lett.* **101**, 097207.
Bao, W., Pagliuso, P. G., Sarrao, J. L., Thompson, J. D., Fisk, Z., Lynn, J. W. & Erwin, R. W. (2000). *Phys. Rev. B*, **62**, R14621–R14624.
Baum, M., Komarek, A. C., Holbein, S., Fernández-Díaz, M. T., André, G., Hiess, A., Sidis, Y., Steffens, P., Becker, P., Bohatý, L. & Braden, M. (2015). *Phys. Rev. B*, **91**, 214415.
Bertaut, E. F. (1968). *Acta Cryst.* A**24**, 217–231.
Biffin, A., Johnson, R. D., Choi, S., Freund, F., Manni, S., Bombardi, A., Manuel, P., Gegenwart, P. & Coldea, R. (2014). *Phys. Rev. B*, **90**, 205116.
Biffin, A., Johnson, R. D., Kimchi, I., Morris, R., Bombardi, A., Analytis, J. G., Vishwanath, A. & Coldea, R. (2014). *Phys. Rev. Lett.* **113**, 197201.
Blanco, J. A., Fåk, B., Ressouche, E., Grenier, B., Rotter, M., Schmitt, D., Rodríguez-Velamazán, J. A., Campo, J. & Lejay, P. (2010). *Phys. Rev. B*, **82**, 054414.
Brown, I. D. & McMahon, B. (2002). *Acta Cryst.* B**58**, 317–324.
Campbell, B. J., Stokes, H. T., Tanner, D. E. & Hatch, D. M. (2006). *J. Appl. Cryst.* **39**, 607–614.
Coldea, R., Tennant, D. A., Cowley, R. A., McMorrow, D. F., Dorner, B. & Tylczynski, Z. (1996). *J. Phys. Condens. Matter*, **8**, 7473–7491.
Damay, F., Martin, C., Hardy, V., Maignan, A., André, G., Knight, K., Giblin, S. R. & Chapon, L. C. (2010). *Phys. Rev. B*, **81**, 214405.
Gallego, S. V., Perez-Mato, J. M., Elcoro, L., Tasci, E. S., Hanson, R. M., Momma, K., Aroyo, M. I. & Madariaga, G. (2016). *J. Appl. Cryst.* **49**, 1750–1776.
Glazer, A. M., Aroyo, M. I. & Authier, A. (2014). *Acta Cryst.* A**70**, 300–302.
Hanson, R. (2013). *Jmol: An Open-Source Java Viewer for Chemical Structures in Three Dimensions.* http://www.jmol.org/.
Harris, A. B. (2007). *Phys. Rev. B*, **76**, 054447.
Harris, A. B., Kenzelmann, M., Aharony, A. & Entin-Wohlman, O. (2008). *Phys. Rev. B*, **78**, 014407.
Herpin, A. & Meriel, P. (1961). *J. Phys. Radium*, **22**, 337–348.
Hwang, S. R., Li, W.-H., Lee, K. C., Lynn, J. W. & Wu, C.-G. (2000). *Phys. Rev. B*, **62**, 14157–14163.
International Union of Crystallography (2015). *Commission on Magnetic Structures*. http://www.iucr.org/iucr/commissions/magnetic-structures.
Izyumov, Y. A., Naish, V. E. & Ozerov, R. P. (1991). *Neutron Diffraction of Magnetic Materials.* Dordrecht: Kluwer Academic Publishers.
Janner, A. & Janssen, T. (1980). *Acta Cryst.* A**36**, 408–415.
Janoschek, M., Fischer, P., Schefer, J., Roessli, B., Pomjakushin, V., Meven, M., Petříček, V., Petrakovskii, G. & Bezmaternikh, L. (2010). *Phys. Rev. B*, **81**, 094429.
Janssen, T., Chapuis, G. & de Boissieu, M. (2007). *Aperiodic Crystals: From Modulated Phases to Quasicrystals.* IUCr Monographs in Crystallography, No. 20. Oxford University Press.
Janssen, T. & Janner, A. (2014). *Acta Cryst.* B**70**, 617–651.
Janssen, T., Janner, A., Looijenga-Vos, A. & de Wolff, P. M. (2006). *International Tables for Crystallography*, Vol. C, *Mathematical and Physical Chemistry*, edited by E. Prince, pp. 907–955. Dordrecht: Kluwer Academic Publishers.
Johnson, R. D., Cao, K., Chapon, L. C., Fabrizi, F., Perks, N., Manuel, P., Yang, J. J., Oh, Y. S., Cheong, S. W. & Radaelli, P. G. (2013). *Phys. Rev. Lett.* **111**, 017202.
Keller, L., White, J. S., Frontzek, M., Babkevich, P., Susner, M. A., Sims, Z. C., Sefat, A. S., Rønnow, H. M. & Rüegg, Ch. (2015). *Phys. Rev. B*, **91**, 020409.
Kenzelmann, M., Harris, A. B., Jonas, S., Broholm, C., Schefer, J., Kim, S. B., Zhang, C. L., Cheong, S.-W., Vajk, O. P. & Lynn, J. W. (2005). *Phys. Rev. Lett.* **95**, 087206.
Kenzelmann, M., Lawes, G., Harris, A. B., Gasparovic, G., Broholm, A., Ramirez, P., Jorge, G. A., Jaime, M., Park, S., Huang, Q., Shapiro, A. Y. & Demianets, L. A. (2007). *Phys. Rev. Lett.* **98**, 267205.
Kim, J.-H., Jain, A., Reehuis, M., Khaliullin, G., Peets, D. C., Ulrich, C., Park, J. T., Faulhaber, E., Hoser, A., Walker, H. C., Adroja, D. T., Walters, A. C., Inosov, D. S., Maljuk, A. & Keimer, B. (2014). *Phys. Rev. Lett.* **113**, 147206.
Lemoine, P., Vernière, A., Venturini, G., Marêché, J. F., Capelli, S. & Malaman, B. (2012). *J. Magn. Magn. Mater.* **324**, 2937–2952.
Litvin, D. B. (2013). *Magnetic Group Tables: 1-, 2- and 3-Dimensional Magnetic Subperiodic Groups and Magnetic Space Groups.* Chester: International Union of Crystallography. http://www.iucr.org/publ/978-0-9553602-2-0.
Madariaga, G. (2005). *International Tables for Crystallography*, Vol. G, *Definition and Exchange of Crystallographic Data*, 1st ed., ch. 4.3, p. 270. Dordrecht: Kluwer Academic Publishers.
Makarova, O. L., Tsvyashchenko, A. V., Andre, G., Porcher, F., Fomicheva, L. N., Rey, N. & Mirebeau, I. (2012). *Phys. Rev. B*, **85**, 205205.
Mannix, D., Coad, S., Lander, G. H., Rebizant, J., Brown, P. J., Paixão, J. A., Langridge, S., Kawamata, S. & Yamaguchi, Y. (2000). *Phys. Rev. B*, **62**, 3801–3810.
Manuel, P., Chapon, L. C., Todorov, I. S., Chung, D. Y., Castellan, J.-P., Rosenkranz, S., Osborn, R., Toledano, P. & Kanatzidis, M. G. (2010). *Phys. Rev. B*, **81**, 184402.
Marty, K., Simonet, V., Ressouche, E., Ballou, R., Lejay, P. & Bordet, P. (2008). *Phys. Rev. Lett.* **101**, 247201.
Penc, B., Gerischer, S., Hoser, A. & Szytuła, A. (2012). *J. Magn. Magn. Mater.* **324**, 657–659.
Perez-Mato, J. M., Gallego, S. V., Tasci, E. S., Elcoro, L., de la Flor, G. & Aroyo, M. I. (2015). *Annu. Rev. Mater. Res.* **45**, 217–248.
Perez-Mato, J. M., Ribeiro, J. L., Petříček, V. & Aroyo, M. I. (2012). *J. Phys. Condens. Matter*, **24**, 163201.
Petříček, V., Dušek, M. & Palatinus, L. (2014). *Z. Kristallogr.* **229**, 345–352.
Petříček, V., Eigner, V., Dušek, M. & Cejchan, A. (2016). *Z. Kristallogr. Cryst. Mater.* **231**, 301–312.
Petříček, V., Fuksa, J. & Dušek, M. (2010). *Acta Cryst.* A**66**, 649–655.
Prokeš, K., Petříček, V., Ressouche, E., Hartwig, S., Ouladdiaf, B., Mydosh, J. A., Hoffmann, R. D., Huang, Y.-K. & Pöttgen, R. (2014). *J. Phys. Condens. Matter*, **26**, 122201.
Reehuis, M., Ulrich, C., Maljuk, A., Niedermayer, Ch., Ouladdiaf, B., Hoser, A., Hofmann, T. & Keimer, B. (2012). *Phys. Rev. B*, **85**, 184109.
Rodríguez-Carvajal, J. (1993). *Phys. B Condens. Matter*, **192**, 55–69.
Rodriguez-Carvajal, J. & Bouree, F. (2012). *Eur. Phys. J. Web Conf.* **22**, 00010.
Rousse, G., Rodríguez-Carvajal, J., Wurm, C. & Masquelier, C. (2013). *Phys. Rev. B*, **88**, 214433.
Scagnoli, V., Huang, S. W., Garganourakis, M., de Souza, R. A., Staub, U., Simonet, V., Lejay, P. & Ballou, R. (2013). *Phys. Rev. B*, **88**, 104417.
Stokes, H. T. & Campbell, B. J. (2011). *ISO-Mag: Table of Magnetic Space Groups*. *ISOTROPY Software Suite*. http://iso.byu.edu.
Stokes, H. T. & Campbell, B. J. (2014). *ISOCIF: Create or Modify CIF Files*. *ISOTROPY Software Suite*. http://iso.byu.edu.
Stokes, H. T., Campbell, B. J. & van Smaalen, S. (2011). *Acta Cryst.* A**67**, 45–55.
Tokura, Y., Seki, S. & Nagaosa, N. (2014). *Rep. Prog. Phys.* **77**, 076501.
Urcelay-Olabarria, I., Perez-Mato, J. M., Ribeiro, J. L., García-Muñoz, J. L., Ressouche, E., Skumryev, V. & Mukhin, A. A. (2013). *Phys. Rev. B*, **87**, 014419.
Van Smaalen, S. (2007). *Incommensurate Crystallography.* IUCr Monographs in Crystallography, No. 21. Oxford University Press.